

Gigantoproductid shell spiral and microstructure of tertiary layer: evaluation as taxonomical characters

J. Ricardo MATEOS-CARRALAFUENTE^{1,2*} , Ismael CORONADO³ , Pedro CÓZAR²  and Sergio RODRÍGUEZ^{1,2} 

¹ Department of Geodynamics, Stratigraphy and Paleontology, Faculty of Geological Sciences, Complutense University of Madrid, c/ José Antonio Novais, 12, 28040, Madrid, Spain.

² Geosciences Institute (CSIC-UCM), c/ Severo Ochoa 7, 28040 Madrid, Spain.

³ Faculty of Biological and Environmental Sciences, University of Leon, Campus Vegazana s/n, 24071 León, Spain.

*Corresponding author Email: josericm@ucm.es

ABSTRACT: Brachiopod taxonomy is based on descriptions of shell morphology and key characters, but diagenesis generally modifies or erases some of them, hindering brachiopod identification. Brachiopods that are taxonomically related usually present shells with similar appearance but can differ in size (i.e., Rhynchonellata). Some aspects of morphology – for example the angular measurement of the curvature of the shell or details of shell microstructure – could aid taxonomic identification. Gigantoproductids, which lack a robust taxonomy, have the largest shells among brachiopods and are ideal for this kind of study because of their gigantic size and morphological variability. Furthermore, they have a great abundance and worldwide distribution during the mid-Carboniferous. More than 700 samples have been collected from Sierra Morena (Spain), Montagne Noire (France) and Adarouch (Morocco) identifying up to six gigantoproductid genera: *Globosoproductus*, *Semiplanus*, *Kansuella*?, *Latiproductus*, *Gigantoproductus* and *Datangia*. Microstructural features from 170 thin sections belonging to gigantoproductid ventral valves have been studied, and six crystal morphologies have been distinguished within the tertiary layer: subhorizontal, imbricated, crenulated, acicular, short and long columnar morphologies. Moreover, 23 complete shells from all genera have been selected to investigate shell size and curvature. Results from this study emphasise that shell size, curvature and crystal shape are taxa-related. Finally, a remarkable morphological change in the gigantoproductid populations from the western Palaeo-Tethys occurred during the Viséan–Serpukhovian, from thin-shelled genera with subhorizontal morphology (Viséan) to thick-shelled genera with a tertiary layer consisting of long columnar crystals (Serpukhovian). This study proves that microstructure, maximum thickness and shell spiral characterisation are robust characters when applied to gigantoproductid taxonomy, but also have great potential in other brachiopod groups.



KEY WORDS: brachiopod, columnar tertiary layer, crystal morphology, *Gigantoproductus*, taxonomy.

1. Introduction

Brachiopod taxonomy has been developed based on descriptions of shell morphology, but fossil shells, about 95% of the phylum (Williams *et al.* 1996), usually have relatively few taxonomic characters due to taphonomic loss or the characters being obscured by matrix. This lack of preserved characters highlights the need to develop new tools to identify taxonomically significant shell characters. The shell shape, size and thickness are under significant phylogenetic influence in brachiopods (Rudwick 1959; Balthasar *et al.* 2020), as is the microstructure, which has been proposed as a potential character for taxonomic purposes (Motchurova-Dekova 2001; Motchurova-Dekova *et al.* 2002; Radulović *et al.* 2007; Smirnova & Zhegallo 2022) as well as an environmental proxy (Ye *et al.* 2018).

Biologically controlled mineralisation in brachiopods determines the shell morphology and tailored microstructures

(Pérez-Huerta *et al.* 2018), developing a spiral structure from the umbo to the commissure parallel to the sagittal plane, that grows during the lifespan by accretion, adding new material during secretion of the anterior stage (Ackerly 1992; Aldridge 1999; McGhee 2001). The shell spiral does not usually follow a perfect spiral path, varying during the ontogeny (Clark *et al.* 2016). In order to evaluate this variation, a promising tool was developed by Aldridge & Gaspard (2011), which compares the shell outline with a perfect logarithmic spiral. This method was successfully used for calculating the brachiopod ontogenetic age and for determining palaeoseasonal variations in trace elements (Pérez-Huerta *et al.* 2014; Clark *et al.* 2015, 2016; Gaspard *et al.* 2018).

Nevertheless, brachiopod microstructure has been widely studied with different techniques such as petrological microscopy, scanning electron microscopy, electron backscatter diffraction and atomic force microscopy (Williams 1956, 1968; Rush & Chafetz 1990; Motchurova-Dekova 2001; Garbelli 2017; Ye

et al. 2018; Simonet-Roda *et al.* 2019, 2021). Three different layers have been identified in the brachiopod shell: a primary layer with microgranular appearance, usually absent in fossils; a secondary layer with laminar or fibrous microstructure; and a tertiary layer with a columnar microstructure (Williams 1968). The tertiary layer, despite showing the largest crystals, is poorly investigated compared with the secondary layer, which has been widely studied in extant and fossil brachiopods (Griesshaber *et al.* 2007; Radulović *et al.* 2007; Garbelli 2017; Ye *et al.* 2018; Simonet-Roda *et al.* 2019). Ye *et al.* (2018) noted differences in crystal size and shape in the secondary layer between two species of the same genera, associated with environmental factors and ontogeny. Radulović *et al.* (2007) noted size differences of fibres into the secondary layer and proposed a new genus of fossil brachiopod based on its microstructure. Recently, Simonet-Roda *et al.* (2021) studied the microstructure (crystal morphology and crystallographic orientation) of thecideide brachiopods within the context of the group's phylogeny.

During the onset of the main cooling phase of the Last Palaeozoic Ice Age, from the Viséan to Serpukhovian (Carboniferous), gigantoproductids were common and widespread giant brachiopods that inhabited tropical latitudes (Muir-Wood & Cooper 1960; Ferguson 1978; Legrand-Blain *et al.* 1983; Mii *et al.* 2001; Armendáriz *et al.* 2008; Qiao & Shen 2015; Nolan *et al.* 2017). Although this brachiopod group is common in the Upper Mississippian marine fossil record, a robust taxonomy is lacking, despite efforts to establish accurate and exhaustive descriptions. This poor understanding of its taxonomy is mostly due to homoeomorphy and phenotypic plasticity in response to environmental constraints of the group and lack of internal diagnostic shell characters, such as the cardinal process, muscle scars, median septum, brachial ridges and/or brachial cones, obliterated by taphonomic processes. Alternative characters have been used, such as the number of ribs per centimetre, thickness and shell length, specimen width, and curvature (Sarycheva 1928; Prentice 1950, 1956; Sarycheva & Sokolskaya 1952; Muir-Wood & Cooper 1960; Conrad & Legrand-Blain 1971; Legrand-Blain 1973, 1980, 1987; Ferguson 1978; Pattison 1981; Legrand-Blain *et al.* 1983; Zakowa 1985; Lazarev 1990; Brunton *et al.* 1995; Brunton & Lazarev 1997; Tazawa & Miyake 2002; Ibaraki *et al.* 2008; Qiao & Shen 2012; Aretz *et al.* 2019; Pakhnevich 2019).

Among brachiopods, gigantoproductids have one of the largest and thickest shells of all the fossil record (Angiolini *et al.* 2019), which make them exceptionally useful for microstructural studies; unfortunately, however, the microstructure of the group has only been vaguely described in the literature (Mii *et al.* 2001; Armendáriz *et al.* 2008; Angiolini *et al.* 2012, 2019; Nolan 2017).

Here, combined microstructural and shell spiral studies of six gigantoproductid genera are analysed from different geological basins and ages (Viséan to Serpukhovian). The use of these potential tools as taxonomic characters sheds new light on the taxonomy of the group.

1.1. Geological setting

Brachiopods were sampled in Sierra Morena (SE of Iberian Massif, Spain), Montagne Noire (Hérault, SW of Central Massif, France) and Adarouch areas (NE of the Variscan Massif of Morocco) (Fig. 1). In total, 27 stratigraphic sections have been sampled, mainly limestones and marlstones. More than 700 gigantoproductid specimens, both complete and fragmentary, were collected. Sierra Morena samples were collected from 12 sections in the Guadiato and Guadalquivir valley (close to Adamuz): Sierra Boyera, Cerro de Los Pradillos, Alcolea, Sierra de la Estrella, Cantera del Castillo, El Collado, Valdemilano, Fuenteagria, La Lozana, La Caridad, San Antonio and La Urraquilla. In addition, two sections yielding gigantoproductids

have been investigated and sampled from Los Santos de Maimona Basin: Los Santos de Maimona and Cerro Almeña. The Guadiato Valley has been interpreted as an inner platform of Viséan–Westphalian age (Cózar & Rodríguez 1999), Guadalquivir Valley as platform to slope facies with Brigantian to Pendleian age strata (Cózar & Rodríguez 2004; Cózar *et al.* 2006) and Los Santos de Maimona as an inner platform to slope facies (Rodríguez *et al.* 1992). The Southern Montagne Noire is the most northerly sampled area based on seven sections: Tour de Castellás, Roc du Cayla, Roque Redonde, Les Pascales-2, Escandolge-1, Castelsec, La Serre and Escandolge-2, interpreted as shallow platform to slope facies with several olistoliths (Vachard *et al.* 2016, 2017; and references herein). The samples from the southeastern Montagne Noire have a Viséan to Serpukhovian age. In Adarouch, five sections have been sampled: Tizi ben Zizouit, Akerchi-2, Idmarrach-2, Tihela and Akerchi-1. Adarouch facies have been interpreted as part of a foreland basin of late Viséan to Serpukhovian age (Cózar *et al.* 2011). The biostratigraphy of the sections is summarised in Table 1.

1.2. Material and methods

Specimens were carefully cleaned and sectioned in halves from the umbo to the commissure, whenever possible, as some shells were incomplete or had suffered decortication. Each slab was polished with carborundum down to 1200 grain size, and with 1 µm and 0.3 µm alumina powder. Polished sample slabs were scanned to enable digital cross-reference with micrographs obtained by optical techniques, and 270 thin sections were prepared. The material is housed in the palaeontological collections of the Paleontology Area, Complutense University of Madrid (UCM).

A petrographic microscope (LM Leica DMLP) with coupled camera (Leica DC 300) was used to photograph the thin sections with the purpose of characterising the brachiopod microstructure using cross-polarised filters in petrological microscopy.

In addition, natural breakage fragments and polished slabs were studied with scanning electron microscopy (SEM). Polished slabs of the whole gigantoproductid section were etched in 5% HCl solution for 10–15 s. These samples were gold-coated and analysed using a model JEOL 6400 JSM located in the Spanish National Centre for Electron Microscopy of the UCM. A combination of petrological microscopy and SEM was used to evaluate shell preservation and to measure the well-preserved crystals.

Crystal length, width and orientation were measured in each crystal in different regions of the shells. Measurements, in millimetres (mm) and degrees, were made via micrographs of the thin sections using the plug-in ObjectJ 1.03w (Vischer *et al.* 1994) of the open-source ImageJ 1.47v image processing software (Abramoff *et al.* 2004) and the statistics were processed using Originpro2019 software 9.6. More than 10,000 columnar crystals from the tertiary layer of 170 gigantoproductid ventral valve shells were measured in complete and fragmented specimens. Columnar crystal disorientations have been calculated in well-preserved areas of each sample, by comparing all orientations measured with a selected arbitrary reference crystal and measuring the disorientation angle of each crystal relative to the reference crystal.

In addition, each shell spiral was measured in 23 ventral valves, corresponding to complete shells continuous from the umbo to the commissure. Shell spiral coordinates of each valve were obtained outlining the ventral valve using ObjectJ 1.03w plugin in ImageJ, with the concavity of the ventral valve faced down, the umbo at the left and the commissure at the right (brachiopod in life position). Spirals were grouped using a 2D convex hull algorithm with Originpro2019 software 9.6. The shell spiral deviations of 23 samples from this study and 14 samples from the literature were measured using R software V. i386 4.0.3 using the

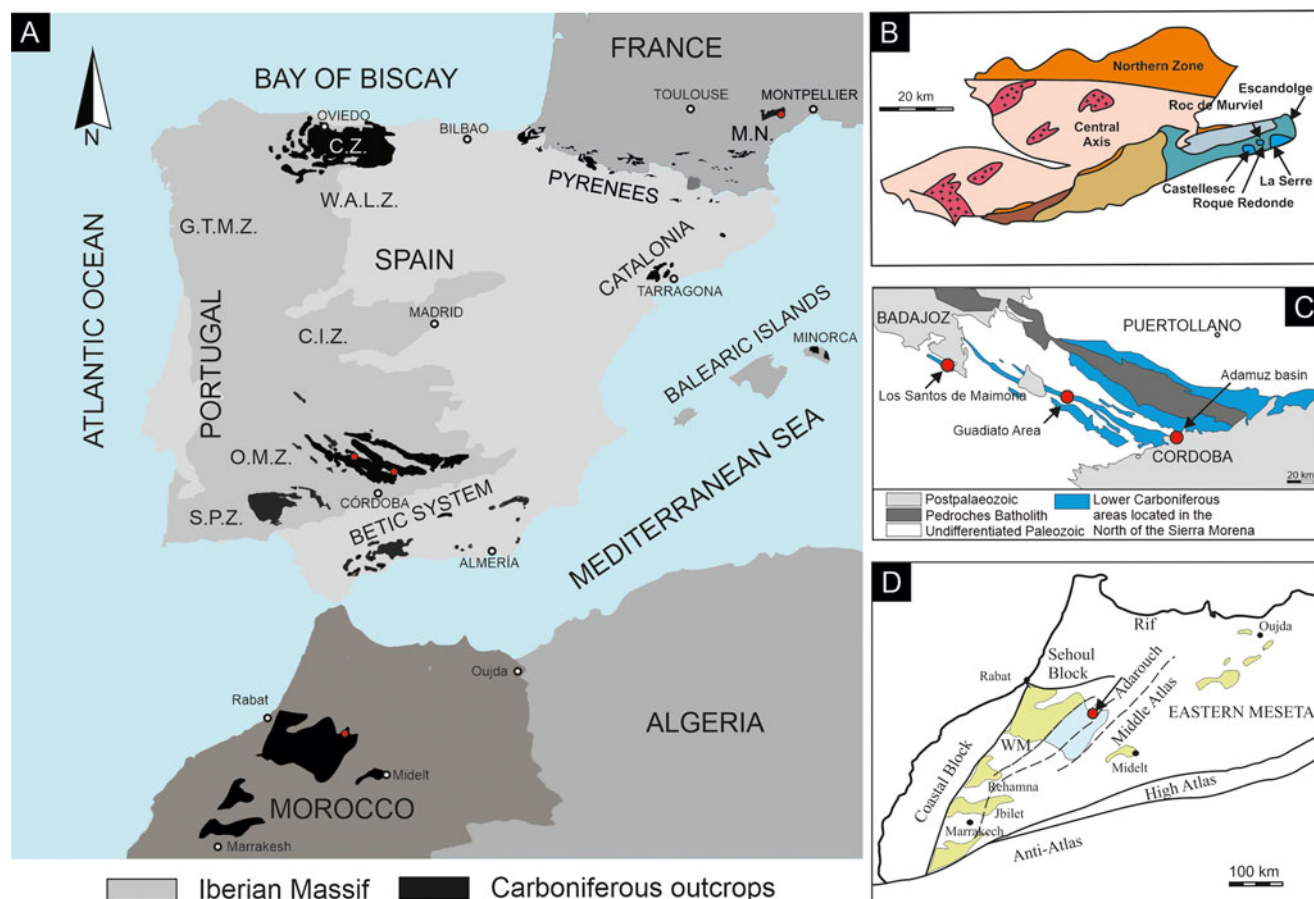


Figure 1 Location maps. (A) Sampled areas (red dots) of the Carboniferous outcrops of France, Morocco and Spain. (B) Montagne Noire sampled outcrops (modified from Vachard *et al.* 2017). (C) Sierra Morena sampled outcrops (modified from Cózar & Rodríguez 1999). (D) Morocco sampled outcrops (modified from Cózar *et al.* 2011).

algorithm developed by Aldridge (1999) and updated in Clark *et al.* (2015).

2. Diagnosis of gigantoproductid specimens

Six genera of gigantoproductids have been identified in the studied outcrops attending to the characters commonly used in the literature (Legrand-Blain 1973; Ferguson 1978), such as shell size, shell thickness, outline shape and ribbing, whose descriptions can provide a general overview on the slight differences observed in the identified gigantoproductids of this study: *Globosoproductus*, Litvinovich & Vorontsova 1983; *Semiplanus*, Sarycheva & Sokolskaya 1952; *Latiproductus*, Sarycheva & Legrand-Blain 1977; *Kansuella?*, Chao 1928; *Gigantoproductus*, Prentice 1950; and *Datangia*, Yang *et al.* 1977.

Globosoproductus resembles *Gigantoproductus* in shape but is smaller in size, 34–57 mm, with a very thin shell, about 1.5–2 mm thick, and rather incurved shells and thinner ribs. *Globosoproductus* occurs in six sections (Sierra Boyera, Alcolea, Cerro Almeña, Los Santos de Maimona (Martínez-Chacon & Legrand-Blain 1992), La Serre and Idmarrach-2) from all areas; late Viséan–Serpukhovian in age (late Asbian–Pendleian).

Semiplanus resembles *Latiproductus* but with shells that are larger, 30–50 mm, and thicker, 3–5 mm, with stronger ribbing and a markedly incurved umbo. *Semiplanus* occurs in four sections (Los Santos de Maimona, Sierra de la Estrella, El Collado and Tizi ben Zizouit) from Sierra Morena and Adarouch; late Viséan in age (late Asbian–Brigantian).

Kansuella? is medium to larger in size, 40–70 mm, with ellipsoidal contours, but the umbo is straight, apparently flatter than

Gigantoproductus and *Datangia* and has rugae towards the commissure. *Kansuella?* occurs in four sections (Les Pascales-2, Castelsec, Escandolge-2 and Tizi ben Zizouit), from Montagne Noire and Adarouch; late Viséan–Serpukhovian in age (late Asbian–Pendleian).

Gigantoproductus shells have a large shell size, 150–250 mm wide from ear to ear, with thickness of 15–22 mm, rounded shape and fine ribbing that becomes more sinusoidal towards the commissure. Two morphotypes have been distinguished in this study: *Gigantoproductus* sp. 1 with a larger and thicker shell and more reticulate ribs than *Gigantoproductus* sp. 2. *Gigantoproductus* sp. 1 occurs in seven sections (Fuenteagria, La Caridad, San Antonio, Akerchi-1 and 2, Idmarrach-2 and Tirhela) from Sierra Morena and Adarouch; Serpukhovian in age (Brigantian–Arnsbergian). *Gigantoproductus* sp. 2 occurs in two sections (Cantera del Castillo and La Urquilla) from Sierra Morena; late Viséan–Serpukhovian in age (late Asbian–Pendleian).

Latiproductus shells are smaller, 30–40 mm, and thinner, 1.5–2.2 mm, than *Gigantoproductus* and with stronger shell convexity; the shell is wider than long with a marked ribbing. *Latiproductus* occurs in six sections (Valdemilano, Fuenteagria, La Lozana, Tour du Castella, Roc du Cayla and Roque Redonde) in Sierra Morena and Montagne Noire; late Viséan–Serpukhovian in age (Brigantian–Pendleian).

Datangia shells resemble *Gigantoproductus* but are slightly smaller in size, 116 mm, and have a more incurved shell, similar shell thickness, 21 mm, although the ribbing is stronger, and with longer and more triangular ears. *Datangia* occurs in three sections (Escandolge-1 and 2 and La Serre) in the Montagne Noire; Serpukhovian in age (Brigantian–Pendleian).

Table 1 Summary of sampled stratigraphic sections and genera assignation.

Outcrop	Sampled area	Age	Reference	Genera	Sedimentology
El Collado	Guadiato	Brigantian	Cózar (2004)	<i>Semiplanus</i>	Wackestone-Packstone
Sierra de la Estrella	Guadiato	Late Asbian– Brigantian	Cózar <i>et al.</i> (2003)	<i>Semiplanus</i>	Wackestone
Cantera del Castillo	Guadiato	Late Asbian– Brigantian	Cózar & Rodríguez (2004)	<i>Gigantoproductus</i> sp.2	Mudstone-Wackestone
San Antonio	Guadiato	Pendleian	Cózar & Rodríguez (2004)	<i>Gigantoproductus</i> sp.1	Marlstone
La Caridad	Guadiato	Pendleian	Cózar & Rodríguez (2004)	<i>Gigantoproductus</i> sp.1	Wackestone
Sierra Boyera	Guadiato	Late Asbian	Cózar & Rodríguez (2000)	<i>Globosoproductus</i>	Wackestone
La Lozana	Guadiato	Pendleian	Cózar & Rodríguez (2004)	<i>Latiproductus</i>	Mudstone-Wackestone
Valdemilano	Guadiato	Brigantian	Cózar <i>et al.</i> (2006)	<i>Globosoproductus</i> , <i>Latiproductus</i>	Mudstone-Wackestone
Alcolea	Guadiato	Late Asbian	Moreno-Eiris <i>et al.</i> 1995	<i>Globosoproductus</i>	Wackestone
Cerro de Los Pradillos	Guadiato	Late Asbian	Cabanás (1963)	<i>Globosoproductus</i>	Mudstone
Fuenteagria	Guadiato	Pendleian	González <i>et al.</i> (2018)	<i>Gigantoproductus</i> sp.1, <i>Latiproductus</i>	Wackestone
La Urraquilla	Guadiato	Pendleian	Cózar <i>et al.</i> (2004)	<i>Gigantoproductus</i> sp.2	Mudstone-Wackestone
Cerro Almeña	Los Santos de Maimona basin	Late Asbian	Rodríguez & Comas-Rengifo (1989)	<i>Globosoproductus</i>	Wackestone
Los Santos de Maimona	Los Santos de Maimona basin	Late Asbian	Rodríguez & Comas-Rengifo (1989)	<i>Globosoproductus</i> , <i>Semiplanus</i>	Wackestone
Roque Redonde	Montagne Noire	Brigantian	Vachard <i>et al.</i> (2016, 2017)	<i>Latiproductus</i>	Wackestone
Castelsec	Montagne Noire	Brigantian– Pendleian	Vachard <i>et al.</i> (2016, 2017)	<i>Kansuella?</i>	Packstone
Escandolge-1	Montagne Noire	Brigantian	Vachard <i>et al.</i> (2016, 2017)	<i>Datangia</i>	Wackestone-Packstone
Escandolge-2	Montagne Noire	Pendleian	Vachard <i>et al.</i> (2016, 2017)	<i>Kansuella?</i> , <i>Datangia</i>	Packstone-Grainstone
La Serre	Montagne Noire	Brigantian	Vachard <i>et al.</i> (2016, 2017)	<i>Datangia</i> , <i>Globosoproductus</i>	Mudstone-Wackestone
Tour du Castellat	Montagne Noire	Brigantian	Vachard <i>et al.</i> (2016, 2017)	<i>Latiproductus</i>	Mudstone-Wackestone
Roc du Cayla	Montagne Noire	Brigantian	Vachard <i>et al.</i> (2016, 2017)	<i>Latiproductus</i>	Mudstone-Wackestone
Les Pascales-2	Montagne Noire	Brigantian	Vachard <i>et al.</i> (2016, 2017)	<i>Kansuella?</i>	Wackestone-Packstone
Idmarrach-2	Adarouch	Pendleian– Arnsbergian	Cózar <i>et al.</i> (2011)	<i>Gigantoproductus</i> sp.1, <i>Globosoproductus?</i>	Wackestone-Packstone
Tirhela	Adarouch	Arnsbergian	Cózar <i>et al.</i> (2011)	<i>Gigantoproductus</i> sp.1	Wackestone
Akerchi-1	Adarouch	Arnsbergian	Cózar <i>et al.</i> (2011)	<i>Gigantoproductus</i> sp.1	Packstone-Grainstone
Akerchi-2	Adarouch	Brigantian	Cózar <i>et al.</i> (2011)	<i>Gigantoproductus</i> sp.1	Packstone-Grainstone
Tizi ben Zizouit	Adarouch	Late Asbian	Cózar <i>et al.</i> (2020)	<i>Semiplanus</i> , <i>Kansuella?</i>	Packstone

3. Results

The results section combines descriptions and measurements made on our material (i.e., from Sierra Morena, Montagne Noire and Adarouch areas), and some specimens from the literature, which have been measured and analysed using the same aforementioned methods.

3.1. Characterisation of the gigantoproductids' ventral valve

Fossil gigantoproductids have concave-convex shells consisting of three layers (Fig. 2): the primary layer in the outer shell is always erased by diagenesis; this is followed by the laminar secondary and the columnar tertiary layers; the tertiary layer is the widest and occupies the innermost portion of the shell. Spiral growth of brachiopods creates a new commissure that thickens and lengthen the shell (Fig. 2). Each stage is separated by a growth line. The growth lines are interruptions or decelerations during the shell growth (*sensu* Hiller 1988), associated with a microstructural change. The growth lines are not perfectly parallel and equidistant from each other, which creates differences in growth of the shell spiral (Gaspard *et al.* 2018). These differences in growth, which correspond to ontogenetic stages, may modify the external shape of the shells in the form of shell spiral deviations.

3.1.1. Morphology of the ventral valve. Gigantoproductids' ventral valves have an ellipsoidal shape, more rounded in *Gigantoproductus* and *Globosoproductus*. In contrast, *Datangia* has triangular ears, which elongate the hinge line and show a more

triangular aspect than *Gigantoproductus*. *Latiproductus* and *Semiplanus* have a narrower ellipse contour, elongated from ear to ear. *Kansuella?* shows an ellipsoidal shape but with a straight edge at the umbo. Some descriptions from the literature have been used for comparisons with other gigantoproductid genera such as *Titanaria*, which resembles *Gigantoproductus* in size and shape but may be differentiated by the morphology of the cardinal process and muscle scars (Muir-Wood & Cooper 1960). On the other hand, *Beleutella* has a smaller size than *Gigantoproductus* and *Titanaria*, is much less incurved, and the ribs are narrow with a low number of spines and more widely spaced (Legrand-Blain 1987).

Besides the distinctive morphological features, size differences (i.e., valve thickness and arc length, also called spiral length) between genera are noticeable, too, and they can be grouped into two clusters (Fig. 3): *Gigantoproductus* and *Datangia* have the largest shells with greater variation in size than *Globosoproductus*, *Latiproductus* and *Semiplanus*. Dimensions among this last cluster are closer with smaller and thinner ventral valves (Fig. 3a). On the other hand, additional genera from literature included in this study (e.g., *Titanaria* and *Belleutela*) exhibit similar dimensions to those genera from the second cluster (i.e., *Globosoproductus*, *Latiproductus* and *Semiplanus*). *Titanaria* occupies an intermediate position with species in both clusters, whereas *Belleutela* and *Kansuella* have similar valve thicknesses, although *Belleutela* is longer.

Shell spiral measurements are summarised in Table 2. Ventral valve length (linear measurement) and the arc length (i.e., length of the shell spiral from the umbo to the commissure) are

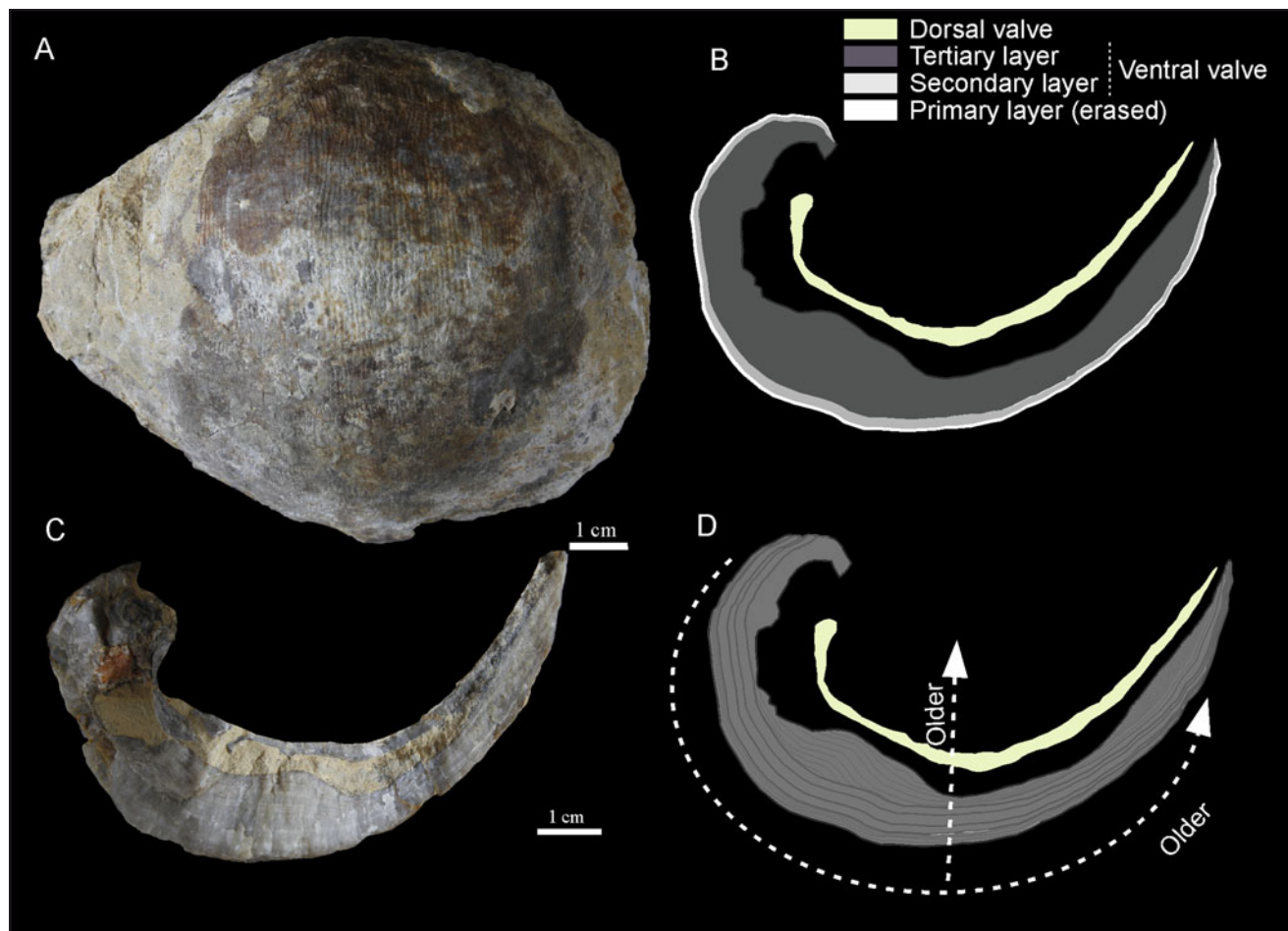


Figure 2 *Gigantoproductus* sp. 1. (A) Outer ventral valve and section view (C). (B) Graphic scheme of the gigantoproductid shell layers situation. (D) Growth vectors of the shell.

measured to identify the larger and smaller genera. *Gigantoproductus* sp. 1 has the largest ventral valve, followed closely by *Datangia*, with a very similar valve thickness (~20 mm). *Gigantoproductus* sp. 2 is smaller and thinner (~12 mm) than *Gigantoproductus* sp. 1 and *Datangia*. *Latiproductus*, *Globosoproductus* and *Semiplanus* show similar size between them and have thinner ventral valves than the previous thick genera; *Semiplanus* is the thickest genera of this cluster.

Differences in shell spiral are due to the incurvation degree (i.e., convexity) of the shell, represented by the (k) parameter. This parameter indicates the valve shape: higher (k) values describe more flattened valves and lower (k) values describe more incurved valves (Table 2). The thicker valves of *Gigantoproductus* sp. 1, *G.* sp. 2 and *Datangia* show similar curvature values (Fig. 3), whereas the thinner valves show more variability. *Globosoproductus* exhibits the most incurved shell of the analysed taxa, followed by *Semiplanus* and *Latiproductus*, which have similar flatness. The theoretical beginning of the spiral is represented by the (a) parameter. Low (a) values indicate a better fitting of the specimen spiral and the theoretical spiral at the beginning of the spiral (Table 2). *Latiproductus* and *Gigantoproductus* sp. 1 have the best fit to a theoretical spiral, followed by *Semiplanus*. *Globosoproductus*, *Datangia* and *Gigantoproductus* sp. 2 show higher (a) values, which corresponds to a considerable distance between the beginning of the theoretical spiral and the real spiral of the ventral valve.

The growth spiral of the brachiopod shells does not perfectly match the idealised theoretical spiral: deviations from the theoretical spiral occur with positive (towards the centre) and negative (outwards from the centre) deflections from the

theoretical trajectory (Fig. 4). When these deviations occur outwards, the spiral (i.e., the external part of valve) is defined as the maxima, whereas if spiral deviations occur inwards the spiral (i.e., the central part of the valve) is defined as the minima. Analysed shell spirals show differences in the magnitude of deviations, with wider and larger ones with 2–4 maxima and minima across the shell, and multiple narrow and smaller ones, which seem more randomly located. Figure 4 shows different spiral deviation plots calculated over the outer line of *Gigantoproductus* sp. 1, *Latiproductus* and *Semiplanus* shells of this study and compared with specimens of the same genera from literature. The upper row represents the spiral deviations calculated for collected samples of this study; the lower row represents the spiral deviations calculated from specimens of the literature. Larger deviations of the shell spiral are usually located at the umbo, the middle part of the shell and the final portion of the shell, as shown in *Semiplanus* or *Gigantoproductus meridionalis* specimens.

3.1.2. Ventral valve crystal morphologies. The microstructure of the ventral valve of gigantoproductids is shaped by two crystal morphologies: laminar in the secondary layer and columnar in the tertiary layer. The secondary layer, located at the most external part of the gigantoproductid brachiopod's shell, is characterised by lath crystals, which constitute the laminar microstructure and are characteristic of the growth lines sandwiched between columnar microstructure into the tertiary layer. Moreover, six crystal morphologies have been identified in the tertiary layer of the ventral valve, characterised by a column-like crystal morphology. Six columnar morphologies have been identified in the tertiary layer associated with crystal shape differences: long

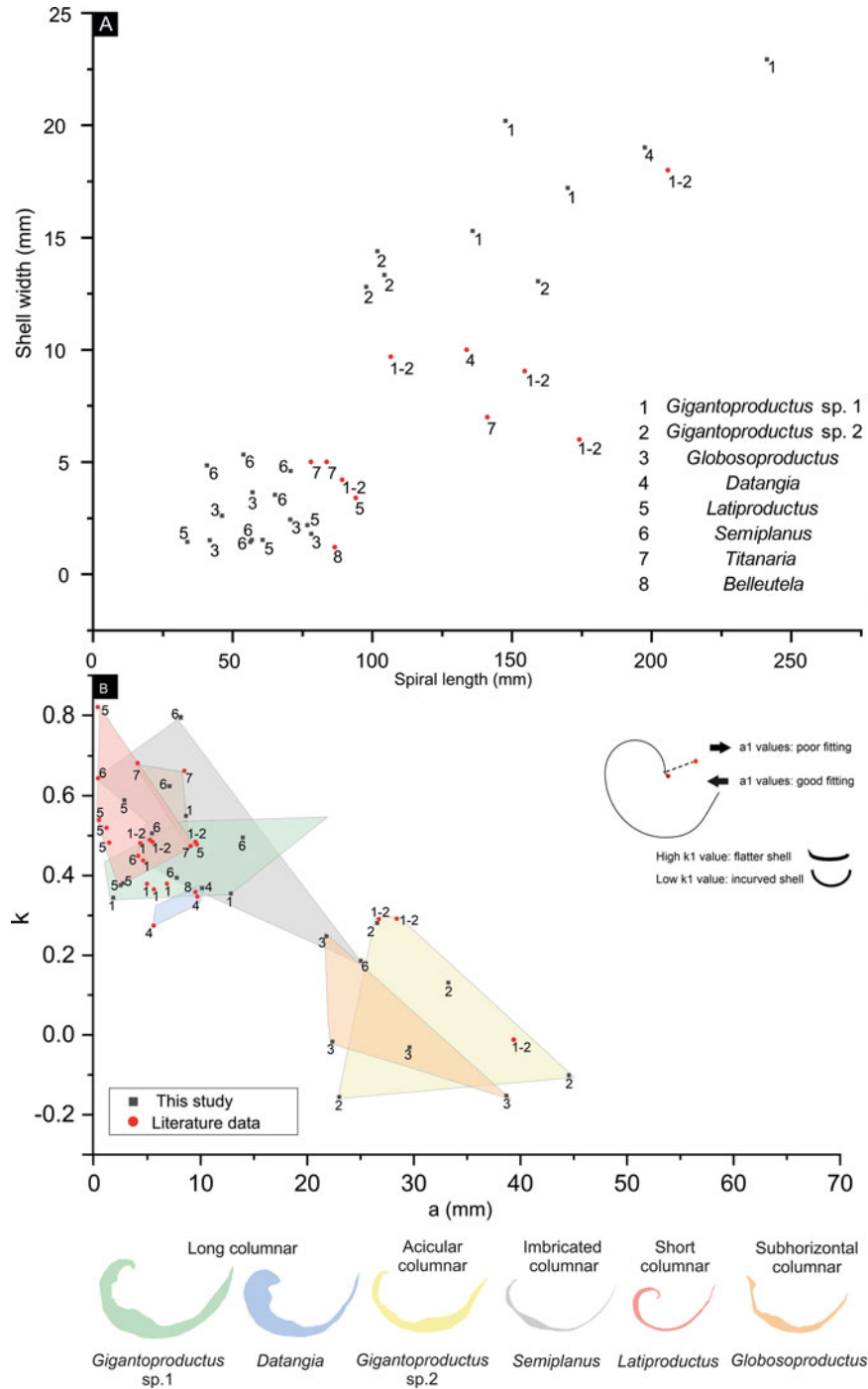


Figure 3 (A) Dispersion graph comparing the shell length/width of different gigantoproductid genera. (B) Dispersion graph showing the (*a*) and (*k*) parameters of different gigantoproductid genera from this study (grey squares) and from literature (red dots). (*a*) is the distance from the spiral to the first point measured in the umbo and (*k*) indicates the convexity of the shell; the higher values describe a flatter shell and the low values high incurved shells. Schematic shell sections from the studied genus and its associated microstructure (right bottom) have been projected in the upper graph.

columnar, short columnar, acicular columnar, imbricated columnar, subhorizontal columnar and crenulated (Fig. 5).

Each crystal morphology identified varies in shape and size between different genera or morphotypes in the case of *Gigantoproductus* (Figs 5 and 6; Table 3). The tertiary layer in *Gigantoproductus* sp. 1 and *Datangia* is characterised by long columnar crystals, whereas *Gigantoproductus* sp. 2 has acicular columnar crystals. *Globosoproductus* exhibits subhorizontal columnar crystals, whereas imbricated crystals are characteristic in *Semiplanus*. The short columnar morphology is found in *Latiproductus* specimens and *Kansuella?* is characterised by columns with crenulated appearance. Moreover, other microstructures appear in *Kansuella?*, such as columns similar to the subhorizontal

columns of *Globosoproductus* and columnar crystals similar to *Latiproductus* but sandwiched into the subhorizontal-like columnar crystals. This feature makes *Kansuella?* unsuitable for microstructural comparisons with other genera from this study and their specimens have not been measured.

Columnar crystals in *Gigantoproductus* sp. 1, *Datangia* and *Latiproductus* have a higher width/length ratio and straighter crystal contacts than *Semiplanus*, *Globosoproductus* and *Gigantoproductus* sp. 2, which have more elongated columns and undulating contacts between crystals. Microstructural features and crystal measurements are summarised in Table 3. *Gigantoproductus* sp. 1 and *Datangia* have the highest average crystal width, with the longest crystal measurement (9.55 mm).

Table 2 Shell measurements from analysed gigantoproductid taxa. Abbreviations: Max length = Maximum length; arc length = length of the shell spiral; n = number of digitised points; mm dig^{-1} = average point distance in mm; Max thickness = maximum thickness of the shell; a = distance in mm of the beginning of the real and theoretical spiral; k = shell curvature.

Taxa from this study	Measurements								
	Max length	Arc length	n	mm dig^{-1}	Max thickness (mm)	a	k	Error	Microstructure
<i>Semiplanus</i>	29.8	40.83	273	0.15	4.85	7.76	0.39	0.15	Imbricated column
<i>Semiplanus</i>	56.45	70.83	188	0.38	4.59	25.03	0.19	0.18	
<i>Semiplanus</i>	36.75	53.9	250	0.22	5.33	5.45	0.51	0.44	
<i>Semiplanus</i>	48.14	65.21	180	0.36	3.54	13.96	0.49	1.08	
<i>Semiplanus</i>	49.6	56.39	318	0.18	4.83	6.39	1.20	0.30	
<i>Semiplanus</i>	47.84	56.91	299	0.19	4.91	8.09	0.79	0.19	
<i>Globosoproductus</i>	34.09	41.85	115	0.36	1.52	22.38	-0.02	0.40	Subhorizontal column
<i>Globosoproductus</i>	47.65	57.15	178	0.32	3.65	29.60	-0.03	0.28	
<i>Globosoproductus</i>	42.01	46.22	109	0.42	2.61	13.01	0.74	0.32	
<i>Globosoproductus</i>	57.59	70.69	147	0.48	2.43	38.70	-0.15	0.53	
<i>Globosoproductus</i>	60.01	78.13	198	0.39	1.8	21.81	0.25	0.27	
<i>Datangia</i>	101.55	197.57	676	0.29	19.01	10.20	0.37	1.01	Long column
<i>Gigantoproductus</i> sp.1	165.17	241.34	426	0.57	22.93	7.06	0.60	1.30	Long column
<i>Gigantoproductus</i> sp.1	82.54	147.66	647	0.23	20.19	12.84	0.35	0.42	
<i>Gigantoproductus</i> sp.1	90.79	170.07	468	0.4	17.2	1.79	0.34	0.07	
<i>Gigantoproductus</i> sp.1	86.42	135.95	552	0.25	15.29	8.47	0.54	0.79	
<i>Gigantoproductus</i> sp.2	77.57	101.9	254	0.4	14.39	33.25	0.13	0.48	Needle-shape column
<i>Gigantoproductus</i> sp.2	82.27	104.35	287	0.36	13.33	63.72	-0.42	0.16	
<i>Gigantoproductus</i> sp.2	98.19	159.35	389	0.41	13.05	26.77	0.29	1.26	
<i>Gigantoproductus</i> sp.2	51.7	97.79	226	0.43	12.8	23.02	-0.16	0.39	
<i>Latiproductus</i>	39.83	76.75	456	0.17	2.19	2.70	0.38	0.32	Short column
<i>Latiproductus</i>	24.21	33.83	430	0.08	1.43	2.97	0.60	0.25	
<i>Latiproductus</i>	31.38	60.75	360	0.17	1.53	2.51	0.37	0.18	

Literature taxa	Max length	Arc length	n	mm dig^{-1}	Max thickness (mm)	a	k	Error	Author
<i>Gigantoproductus auritus</i>	78.26	130.92	309	0.42	–	9.52	0.48	1.07	Legrand-Blain (1973)
<i>Gigantoproductus meharezensis</i>	109.52	155.89	395	0.39	2.20	1.25	0.44	0.04	
<i>Gigantoproductus subokensis</i>	55.31	89.24	278	0.32	4.20	5.52	0.48	0.54	
<i>Gigantoproductus flamandi</i>	114.89	205.81	404	0.51	18.00	26.74	0.29	1.10	
<i>Gigantoproductus meridionalis</i>	110.3	174.17	217	0.8	6.00	28.41	0.29	0.76	
<i>Titanaria africana</i>	53.36	78.04	198	0.39	5.00	4.10	0.68	0.57	Legrand-Blain (1987)
<i>Titanaria africana 2</i>	55.55	83.63	173	0.48	5.00	9.06	0.47	0.31	
<i>Belleutela</i>	53.28	86.59	153	0.57	1.20	9.52	0.36	1.11	
<i>Datangia pyrenaesus</i>	74.79	133.8	258	0.52	10.00	9.72	0.35	0.87	
<i>Titanaria horrendensis</i>	97.56	141.23	349	0.4	7.00	8.49	0.66	1.44	
<i>Latiproductus</i>	63.03	94.15	181	–	3.40	9.67	0.48	0.21	Williams <i>et al.</i> (2007)
<i>Semiplanus</i>	55.39	93.55	264	0.35	–	4.14	0.45	0.81	Muir-Wood & Cooper (1960)
<i>Gigantoproductus</i>	91.89	154.56	283	0.55	9.05	5.38	0.49	0.94	Qiao & Shen (2012)
<i>Gigantoproductus giganteus</i>	77.03	106.56	188	0.57	9.69	39.58	-0.02	0.71	

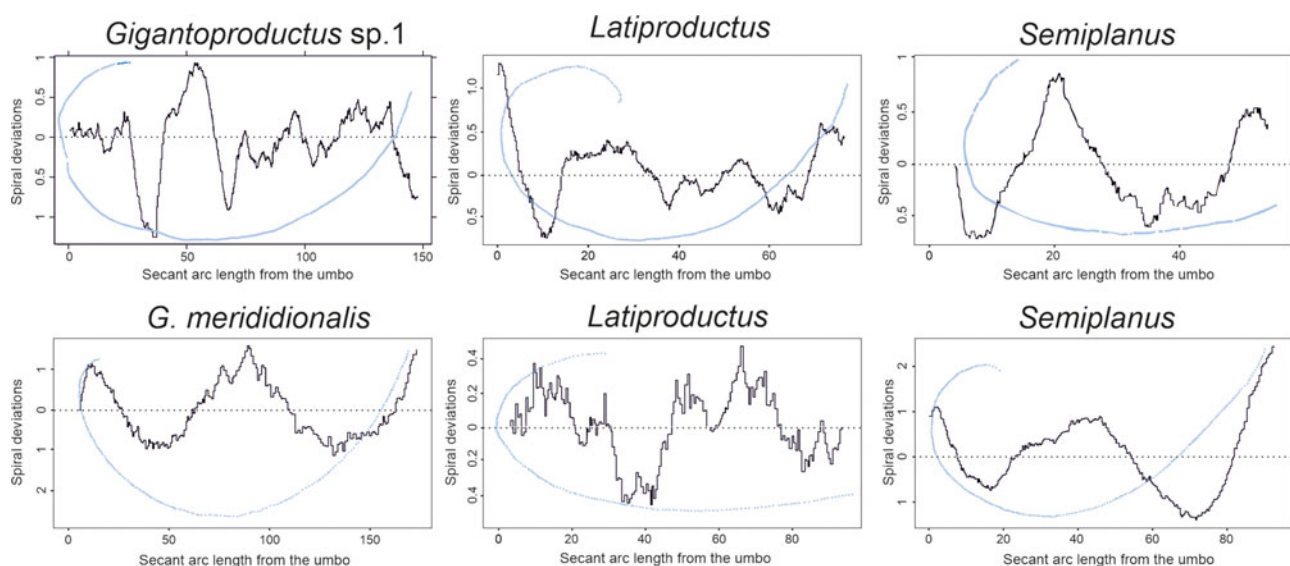


Figure 4 Deviations of the shell spiral in three gigantoproductid genera (top) compared with equivalent genera from the literature (bottom).

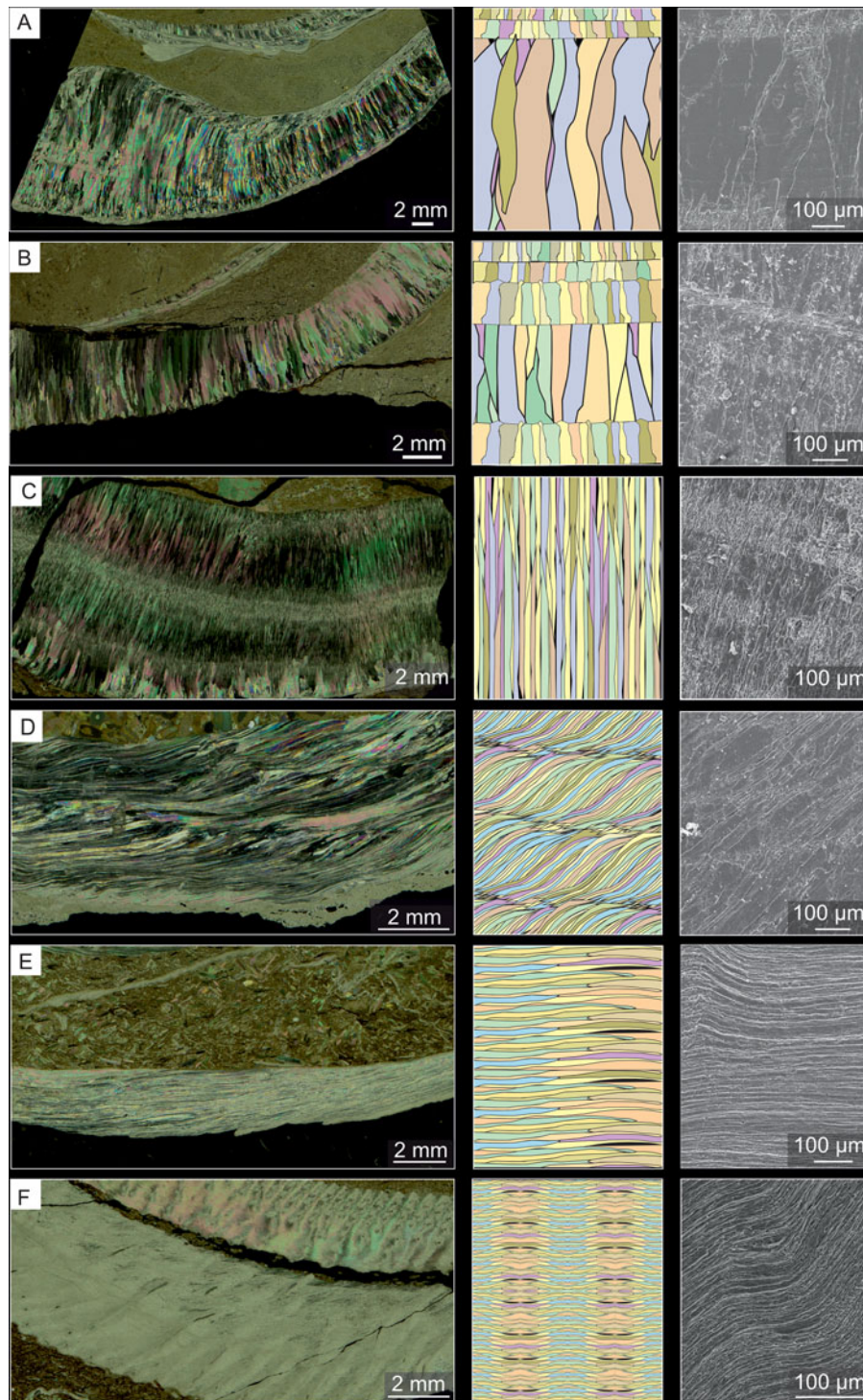


Figure 5 Six columnar morphologies shown under petrological microscopy, synthetic diagram of the crystals and SEM images. Images correspond with transverse sections from the umbo to the commissure. (A) Long columnar morphology of the thick and thin regions in *Gigantoproductus* sp.1. (B) Short columnar morphology of the thick and thin regions in *Latiproductus*. (C) Acicular columnar morphology of the thick region in *Gigantoproductus* sp.2. (D) Imbricated morphology of the thin region in *Semiplanus*. (E) Subhorizontal morphology of the thick region in *Globosoproductus*. (F) Crenulated morphology of the thick region in *Kansuella?*.

Gigantoproductus sp. 2 exhibits a higher average crystal length than *Gigantoproductus* sp. 1, but they are narrower in width. *Latiproductus* and *Globosoproductus* show similar average crystal length whereas *Globosoproductus* has narrower crystals. *Semiplanus* has the highest average crystal length but narrower crystals than the rest of the genera except *Globosoproductus*. *Kansuella?* has a crenulated microstructure in the tertiary layer (Fig. 5).

3.1.3. Intra-shell crystal size variations. Crystal length and width of each morphology have been measured across the whole shell profile from the umbo to the commissure. Crystals

have been grouped into five regions as a function of their relative position in the gigantoproductid ventral valve. The five shell regions were defined based on differences in growth line spacing into the ventral valve, and are named as umbonal (U), thick (Tk), thin (T), inner-thick (ITk) and inner-thin (IT) regions. U-region corresponds to the umbonal part of the shell; Tk-region corresponds to the middle part of the shell, where the shell and the growth line spacing are wider; T-region corresponds to the thinner part of the shell until the commissure, where the growth line spacing decreases; the ITk- and IT-regions correspond to the

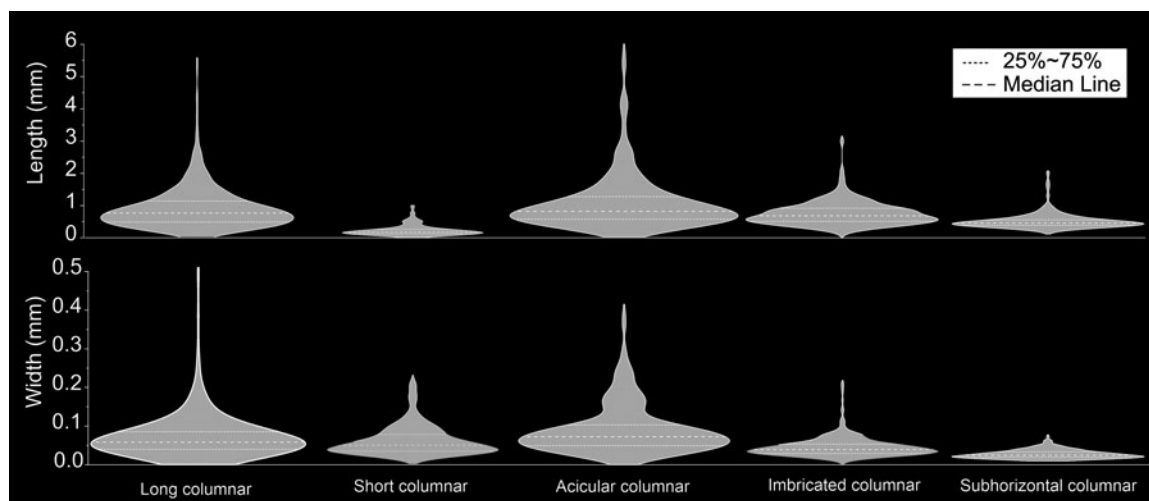


Figure 6 Violin plots (bottom) with the column length and width from studied genera.

innermost parts of Tk- and T-regions respectively, where the growth line spacing decreases progressively. This methodology has been extended in this study by measuring the crystal column length and width of each region in five studied gigantoproductid genera (*Globosoproductus*, *Semiplanus*, *Latiproductus*, *Datangia* and *Gigantoproductus*) to compare microstructural differences (Fig. 7).

Each crystal morphology shows differences in length and width at different shell regions (Fig. 7; Table 4). In all morphologies the Tk-region usually has the longest crystals followed by the T-region and U-region. The ITk- and IT-regions have the shortest crystal column. The crystal width describes a similar trend to crystal length but shows much less size variability. The big and acicular columnar morphologies, which belong to the thickest and biggest shells, show more crystal size variation than the smaller shell morphologies, while the imbricated morphology shows more uniform crystal size across the shell and the subhorizontal morphology shows similar width within the shell regions.

3.1.4. Crystal disorientation in the ventral valve. Crystal disorientations were measured in each crystal morphology of the tertiary layer of the gigantoproductid genera. Generally, crystals show low levels of disorientation regardless of crystal morphologies. Five histograms are plotted to compare crystal disorientation between genera (Fig. 7). A random distribution function was plotted in each histogram to help to compare the disorientation degree in each genus.

All the histograms (Fig. 7) show a Gaussian constrained distribution (i.e., lower standard deviation) in contrast to the random distribution function. The larger and thicker shells, those in *Gigantoproductus* and *Datangia*, show higher crystal disorientation than the thinner shelled *Latiproductus*, *Globosoproductus* and *Semiplanus*. *Gigantoproductus* sp. 1 and *Datangia* present highest disorientation (e.g., mean $\sim 18^\circ$) than other genera (e.g., mean $\sim 9^\circ$ in *Semiplanus*). Additionally, disorientation of well-preserved compared with poorly preserved areas of *Semiplanus* samples were plotted. Widespread disorientation values of the poorly preserved areas were very similar to the random distribution function and broader than well-preserved areas, which show constrained values (from 0° to 48°).

4. Discussion

Gigantoproductid taxonomy is based on descriptions of shell morphological features and key characters of the internal shell surface, such as the morphology of the cardinal process, the muscle scars, or the presence/absence of the brachial cones

(Sarycheva 1928; Prentice 1950, 1956; Sarycheva & Sokolskaya 1952; Muir-Wood & Cooper 1960; Ferguson 1978; Legrand-Blain 1980, 1985, 1987; Legrand-Blain *et al.* 1983; Zakowa 1985; Aretz *et al.* 2019). Homoeomorphy is challenging in all brachiopod studies (Muir-Wood & Cooper 1960), but in gigantoproductids it is complex due to the marked similarities between genera, as Williams *et al.* (2007) noted. Accordingly, other characters have become more significant: shell size and thickness; shell morphology; ribbing density; and shell curvature (Prentice 1956; Legrand-Blain 1973, 1980, 1987; Legrand-Blain *et al.* 1983). In the current study, less than 5 % of specimens preserve one or two of these internal shell characters not hidden by the matrix, but all of them show microstructural features, shell thickness, and complete specimens provide information about spiral and shell length, despite being embedded in matrix or fragmented.

4.1. Gigantoproductid shell size and microstructure through time

Gigantoproductid shells (Fig. 2) have long and thick shells (Muir-Wood & Cooper 1960), longer than any other brachiopods. This is an advantageous feature for palaeoenvironmental and palaeoclimatic studies (e.g., microstructural and geochemical studies), because shell size, thickness or microstructural features are larger than other brachiopod shells (helping microsampling and measuring). Muir-Wood & Cooper (1960) classified productids by their size: under 20 mm are considered small, 20–50 mm are medium size, over 50 mm are called large, and larger than 150 mm are gigantic. In this study, *Latiproductus*, *Semiplanus*, *Kansuella?* and *Globosoproductus* would be considered large in this classification, whereas *Gigantoproductus* and *Datangia* would be considered gigantic.

Figure 3 shows a correlation between the maximum thickness and the arc length of the shell. Longer genera such as *Gigantoproductus* sp. 1 have thicker shells. This is reasonable because during shell growth (in length) the commissure is thickened with a new calcite layer, and so on. It is noticeable that larger genera have more size variation and are clustered for a gap in size from the thin-shelled genera, which are closely grouped. *Latiproductus* varies more in length than in thickness, in contrast to *Semiplanus*. Furthermore, *Globosoproductus* is in an intermediate position. *Gigantoproductus* sp. 1 and *G.* sp. 2 have similar size variability, with *G.* sp. 1 being larger and thicker. It should be highlighted that thick-shelled genera, such as *Gigantoproductus* and *Datangia*, are more common during the Serpukhovian than thin-shelled taxa (*Globosoproductus* and *Latiproductus*), which are more common during the Viséan (Fig. 8; Table 1).

Table 3 Characterisation of microstructural elements and measurements in the analysed gigantoproductids. Abbreviation: S.D. = standard deviation.

Genus	Microstructure	Shell type	Crystal shape	Crystal contact	Length (mean) mm	S.D.	Width (mean) mm	S.D.	Orientation in respect to shell surface
<i>Gigantoproductus</i> sp.1	Long columnar	Thick	Column	Straight	\bar{x} : 0.42 (0.01–9.55)	0.5	\bar{x} : 0.07 (0.01–3.36)	0.1	Sub-perpendicular
<i>Datangia</i>									Sub-perpendicular
<i>Gigantoproductus</i> sp.2	Acicular columnar	Thick	Elongated column	Wavy	\bar{x} : 0.514 (0.03–6.04)	0.61	\bar{x} : 0.07 (0.01–0.41)	0.05	Sub-perpendicular
<i>Latiproductus</i>	Short columnar	Thin	Column	Straight	\bar{x} : 0.38 (0.03–3.32)	0.5	\bar{x} : 0.05 (0.01–0.44)	0.04	Sub-perpendicular
<i>Globosoproductus</i>	Subhorizontal columnar	Thin	Elongated column	Wavy	\bar{x} : 0.42 (0.15–1.93)	0.26	\bar{x} : 0.02 (0.01–0.07)	0.01	Sub-parallel
<i>Semiplanus</i>	Imbricated columnar	Thin	Elongated column	Wavy	\bar{x} : 0.75 (0.17–3.02)	0.37	\bar{x} : 0.04 (0.01–0.21)	0.02	Inclined
<i>Kansuella?</i>	Crenulated	Thick	Elongated column	Wavy	–	–	–	–	Sub-parallel

Moreover, a microstructural shift of the tertiary layer has been illustrated through time, which is related to the shell thickness.

Gigantoproductid crystal columnar crystal morphology of the tertiary layer (Fig. 5) varies during the Viséan–Serpukhovian (Fig. 8) from a predominantly subhorizontal columnar crystal morphology to sub-perpendicular long column crystals. This means a progressive change in gigantoproductid populations from thin-shelled to thicker-shelled genera. *Globosoproductus*, with subhorizontal morphology, dominated during the late Asbian, followed by the imbricated morphology (*Semiplanus* and *Kansuella?*), which are a little bit thicker than *Globosoproductus* and exhibit less incurved shells. *Gigantoproductus* sp. 2 appears at the end of the late Asbian with thicker shells of the aforementioned genera and a curvature similar to *Globosoproductus* (Fig. 3).

A new microstructure appears during the Brigantian with the development of short columns in the tertiary layer, such as the short columnar morphology present in *Latiproductus* (Fig. 8; Table 1). Crystal columns of this genus show differences with respect to the crystal shape of *Semiplanus* and *Globosoproductus*, the last of these being more elongated than *Latiproductus*. Short column type has a lower length/width ratio, straight crystal contacts and sub-perpendicular crystal orientation to the shell surface. This microstructure occurs also in Pendleian specimens but is less common than taxa with long columnar microstructure (*Gigantoproductus* sp. 1 and *Datangia*).

During the late Brigantian and Pendleian the long columnar morphology in *Gigantoproductus* sp. 1 and *Datangia* are predominant over other microstructures, such as the subhorizontal and short columnar. Acicular microstructure is associated with *Gigantoproductus* sp. 2 and occurs only in two outcrops assigned to the Asbian–lower Brigantian and the Pendleian. *Gigantoproductus* sp. 1 is more common than *Latiproductus* during the Pendleian to Arnsbergian, confirming the dominance of the thicker-shelled genera during the Serpukhovian. *Latiproductus* seems a special case due to its occurrence during the Viséan–Serpukhovian interval in several basins and with similar shell thickness (Fig. 8).

The increasing shell size in gigantoproductids during the Viséan–Serpukhovian has been previously noted by other authors and can be tested by comparing with data in the literature.

In Béchar Basin (Algeria), Legrand-Blain (1987) reported a change in the gigantoproductids assemblages from the Viséan (containing *Datangia*, *Kansuella* and *Latiproductus*) to the Serpukhovian (with *Datangia*, *Gigantoproductus*, *Kansuella*, *Titanaria* and *Latiproductus*). This transition represents a change in gigantoproductids' diversity to a predominance of thicker-shelled genera.

In Stainmore and Northumberland (northern England), Pattinson (1981) reported thin-shelled and thin-ribbed gigantoproductid shells of *Linoprotonia* during the Holkerian and early Asbian, which changed to thicker-shelled gigantoproductids such as *Gigantoproductus maximus*, *Gigantoproductus semiglobosus* and *Gigantoproductus submaximus* during the late Asbian to Brigantian.

In the Zhanpo Formation, southern Shaanxi (China), Qiao & Shen (2012) observed that *Gigantoproductus giganteus* has a smaller shell during the Viséan than in the Serpukhovian. On the other hand, these authors described specimens of *Gigantoproductus* sp. with a shell shape and spiral very similar to the samples of the Guadiato area of this study (Fig. 3).

In Montagne Noire, Aretz *et al.* (2019) described the presence of thinner *Datangia* shells (Viséan, 4–8 mm) than the Serpukhovian *Datangia* samples from this study (shell thickness ~19 mm). Moreover, Aretz *et al.* (2019) provided data about the abundance of *Latiproductus* and *Datangia* (shell thickness 4–8 mm) during the early Brigantian, which changed during the Pendleian to *Kansuella* sp. 1 and *K.* sp. 2 (shell thickness 11–15 mm).

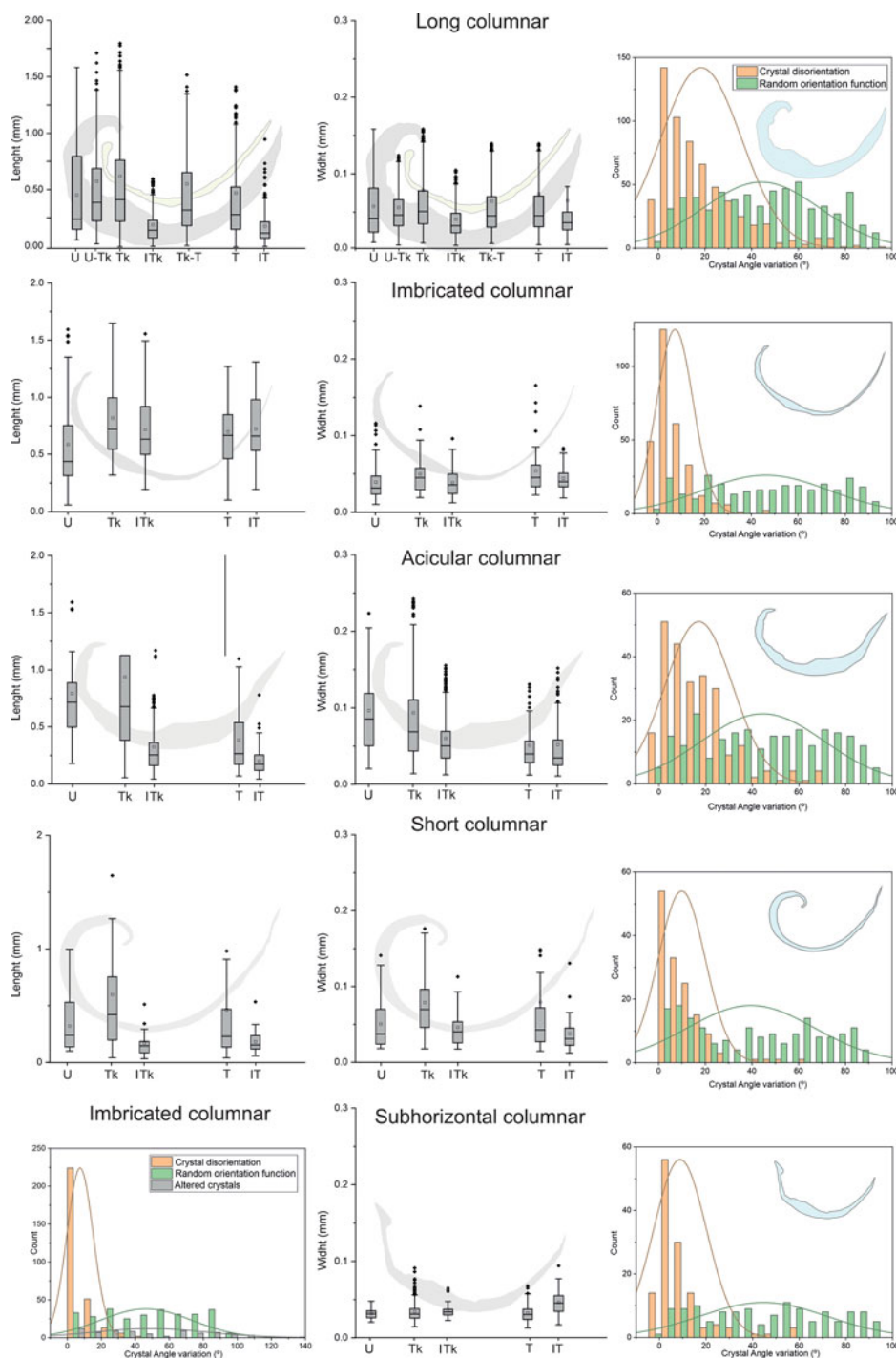


Figure 7 Histograms with intra-shell crystal variations in each shell region of studied gigantoproductid genera (left). Histograms with crystal disorientation in different gigantoproductid genera (right). Crystal disorientation of imbricated morphology (bottom left) compared with a random distribution function.

The shell thickness increase through time, which is latitude independent in extant brachiopods (Watson *et al.* 2012), is a common mechanism in gigantoproductids in the same genera and in the same evolutionary lineage. This trend is also latitude independent in gigantoproductids (China, England, Morocco, Algeria, Montagne Noire and Sierra Morena), although this group inhabited topical–subtropical seas. Balthasar *et al.* (2020) indicated a shell thickening trend in Orthida and shell thinning in Strophomenata and Clitambonitida during the Ordovician–Silurian. These authors suggested different phylogenetic mechanisms of shell thickness variation, which might be related to different strategies in response to environmental changes.

Gigantoproductids are large brachiopods (some of them giants) and possess one of the largest and thickest shells in the fossil record (Angiolini *et al.* 2019). Extant brachiopod species reach a maximum of 70 mm in length (Baumgarten *et al.* 2013) and 0.1–1.2 mm in shell thickness (Foster 1974), whereas gigantoproductids may reach 300–400 mm in width (Muir-Wood & Cooper 1960) and up to 23 mm in maximum ventral valve thickness (Table 2). The size increases observed in this study during the interval between the late Viséan to mid Serpukhovian can fit with one or several of proposed hypotheses about their size, such as available oxygen increasing (shift in tropical forests, Motin *et al.* 2022), primary productivity (Zhang *et al.* 2015), global cold intervals (C1–C2 glacial intervals, Fielding *et al.* 2008),

Table 4 Measurements of crystal length and width in each shell part. Abbreviation: S.D = standard deviation.

Morphology	Part	Length (mm)	Length S.D.	Width (mm)	Width S.D.
Long columnar	U	0.47	0.42	0.06	0.04
	Tk	0.63	0.75	0.08	0.21
	T	0.49	0.64	0.08	0.19
	ITk	0.21	0.25	0.04	0.03
	IT	0.19	0.22	0.07	0.42
Short columnar	U	0.25	0.04	0.05	0.03
	Tk	0.24	0.04	0.07	0.03
	T	0.26	0.28	0.07	0.27
	ITk	0.06	0.01	0.04	0.02
	IT	0.08	0.01	0.03	0.01
Acicular columnar	U	0.78	0.46	0.10	0.06
	Tk	0.93	1.06	0.09	0.11
	T	0.57	0.65	0.05	0.04
	ITk	0.31	0.30	0.06	0.04
	IT	0.19	0.11	0.05	0.04
Imbricated columnar	U	0.59	0.41	0.04	0.02
	Tk	0.83	0.41	0.05	0.03
	T	0.70	0.36	0.05	0.04
	ITk	0.78	0.29	0.04	0.02
	IT	0.63	0.41	0.04	0.02
Subhorizontal columnar	U	–	–	0.021	0.004
	Tk	0.51	0.19	0.023	0.009
	T	–	–	0.021	0.007
	ITk	–	–	0.024	0.006

predation pressure (Vermeij 2016) and photosymbiotic lifestyle of *Gigantoproductus* (Angiolini *et al.* 2019). Variation of gigantoproductid shell morphology and size, and its relationship with environmental factors through this time interval, require further investigation.

4.2. Shell spiral deviations as response to ontogeny

The shell spiral had been used to detect changes during shell ontogeny in extant (Aldridge & Gaspard 2011; Pérez-Huerta *et al.* 2014) and fossil brachiopod shells (Clark *et al.* 2015, 2016). Deviations of the shell spiral are small curvature differences between the shell spiral and the theoretical spiral, which indicate changes in the growth rate (Aldridge & Gaspard 2011) in the form of deviations above (maxima) or below (minima) the line of the theoretical spiral. These changes prove that shell growth is not constant through time and the curvature of the shell varies. There are several factors that could affect brachiopod growth at the biological level (genetic, illness) and/or environmental factors (food availability, shell breakage due to predators or abiotic impacts, temperature, salinity, acidification events, and so on) that cannot be easily linked to deviations of the shell spiral (Aldridge & Gaspard 2011), but in combination with geochemical proxies demonstrate its potential to calculate ontogenetic states and palaeotemperature seasonal variations (Clark *et al.* 2016).

The shell spiral in gigantoproductids shows variations in (*k*) and (*a*) parameters, which seem genus-related, even species-related (Fig. 3). This relation between species and curvature in gigantoproductids was originally shown by Prentice (1956) and Legrand-Blain (1973, 1987) by comparing the curvature of the shell spiral between different species (i.e., graphically outlining the valves).

Figure 3 shows a similar beginning of the spiral fitting and curvature (similar (*a*) and (*k*) values respectively), and low error between *Latiproductus* and *Gigantoproductus* sp. 1, but they have a very different ventral valve thickness. Both genera have a similar microstructure of the tertiary layer, and long

columnar type, with *Gigantoproductus* sp. 1 larger than *Latiproductus*, which may explain the valve thickness differences.

Moreover, *Gigantoproductus* sp. 2 and *Globosoproductus* seem to be a similar case, with proximal (*k*) and (*a*) values and different ventral valve thickness, and *Gigantoproductus* sp. 2 thicker than *Globosoproductus*. Microstructure of the tertiary layer of these two species (Fig. 5) are more elongated (acicular and subhorizontal types) than *Latiproductus* and *Gigantoproductus* sp. 1 (long columnar type). Shell thickness differences in this case may be related to the orientation of the elongation axis of crystals, which is perpendicular to the shell surface in *Gigantoproductus* sp. 2 (acicular type) and parallel to the shell surface in *Globosoproductus* (subhorizontal type). *Semiplanus* exhibits intermediate values between both groups, which may be related to its characteristic microstructure (Fig. 5), whose crystals are tilted relative to the shell surface, an intermediate crystal orientation compared with the other genera (Fig. 7).

Deviations of the shell spiral (Fig. 4) were interpreted as variations in growth (Pérez-Huerta *et al.* 2014; Clark *et al.* 2015, 2016) and, thus, they can be used to infer changes in the growth rate through the ontogeny. Larger and wider deviations in magnitude are possibly related to shell morphology and the smaller deviations seem to be related to the periodical growth increments. The larger spiral deviations in gigantoproductids are usually in the middle part of the shell (Tk-part), which has the largest crystals and thus the highest valve thickness (Table 3; Fig. 7). Thicker shells such as *Gigantoproductus* sp. 1 show larger deviations in magnitude than thinner shells, such as *Latiproductus* or *Semiplanus* (Fig. 4). *Gigantoproductus* sp. 1 and *Latiproductus* show similar (*a*) and (*k*) values (Fig. 3) but higher differences in shell thickness. *Gigantoproductus* sp. 1 valves show the highest maxima and minima in the central part (Tk-region), where the thickness is maximum, about 22 mm. However, *Latiproductus* valves show similar spiral deviations to *Gigantoproductus* sp. 1, where the magnitude is lower due to valve thickness differences. It should be highlighted that larger magnitude deviations of the shell spiral in gigantoproductids are related to valve thickness. Deviations of the shell spiral magnitude generally decrease from the umbo towards the commissure (Fig. 7). It should be noted that thick-shelled taxa (*Gigantoproductus* sp. 1 and *Datangia*) which exhibit very incurved shells have larger crystal disorientations in the tertiary layer, relative to thin-shelled taxa, even if they are strongly incurved as in *Globosoproductus*.

Qualitative curvature information and shell size have been commonly used to distinguish gigantoproductid species (Prentice 1956; Legrand-Blain 1973, 1987; Pattison 1981), and shell size has been applied as a taxonomic character in other brachiopods such as Lingulidae (Kowalewski *et al.* 1997), although *a priori* this group does not show a large variation in shape. This study emphasises that quantitative curvature changes are taxa-related in gigantoproductids and can be a robust taxonomic criterion to cluster mainly thin-shelled brachiopods.

It should be highlighted that the identification by shell measurements of brachiopod shells with large intraspecific variation in size and shape, such as *Terebratalia transversa*, is difficult (Paine 1969), but they can be differentiated from other species by their microstructure, as demonstrated by Griesshaber *et al.* (2007).

4.3. Microstructure as taxonomic criterion

Microstructure as taxonomic character has been evaluated in fossil brachiopod shells (Motchurova-Dekova 2001; Radulović *et al.* 2007; Manceñido & Motchurova-Dekova 2010) to distinguish taxa by comparing dimensions and textures of the secondary layer (e.g., fibres), while Garbelli (2017) reported differences in the columnar crystals of the tertiary layer between Strophomenata and Rhynchonellata.

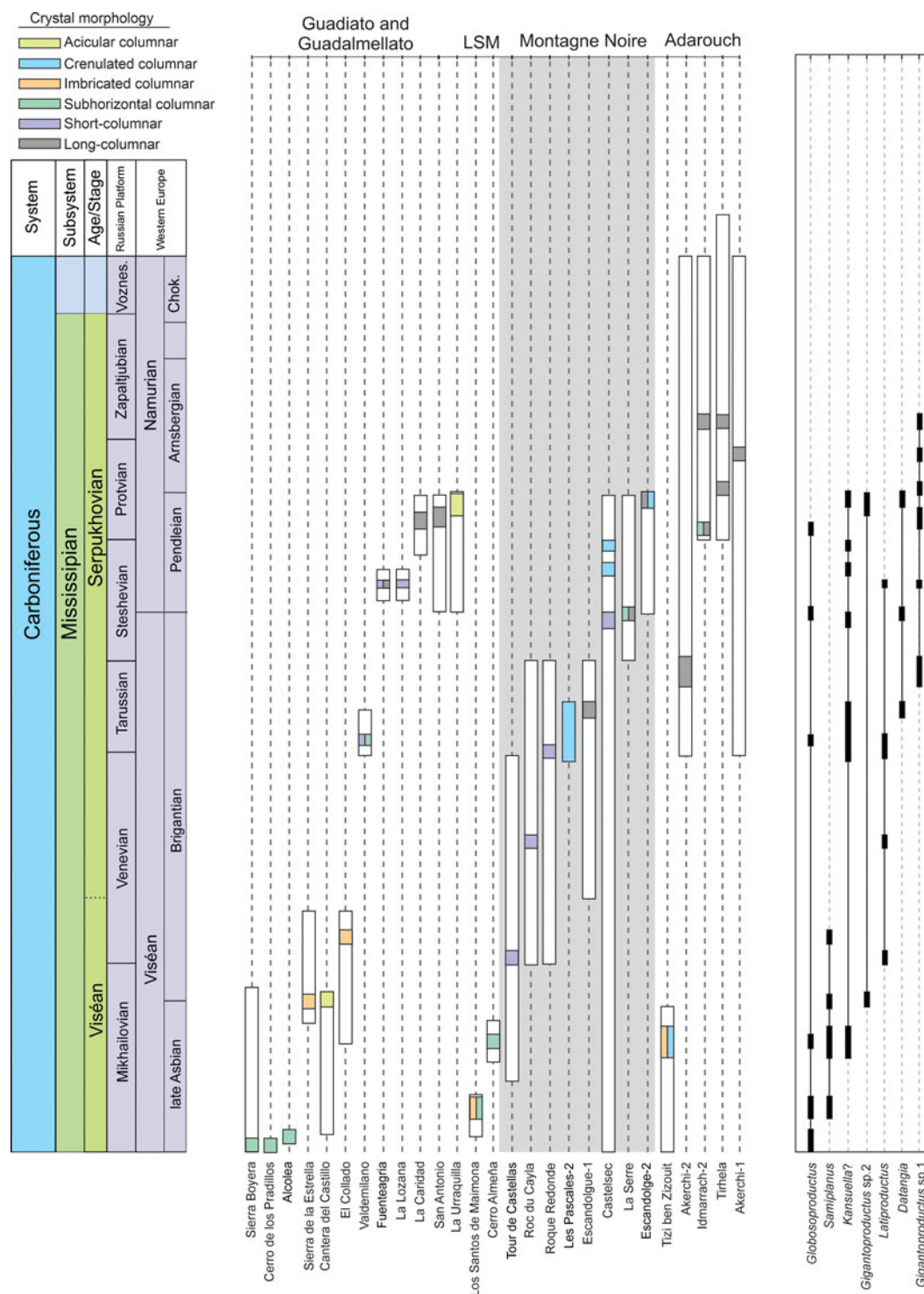


Figure 8 Stratigraphic ranges of sampled sections (coloured bars) and outcrop range (white bars) during the Viséan–Serpukhovian (left). Stratigraphic ranges (black lines) of the genera in this study during the Viséan–Serpukhovian (right).

Gigantoproductids in this study show a crystal microstructure that is taxon-specific (e.g., genera or species). Taxa with elongated crystals (e.g., long columnar and acicular) have thicker valves, more growth lines, larger crystals and higher crystal size variation than *Latiproductus* (short column type), *Globosproductus* (subhorizontal type) and *Simplianus* (imbricated type). Some variability exists, for instance between *Gigantoproductus* sp. 1 and *Datangia*, which have long column type microstructure, but *Gigantoproductus* sp. 1 has larger crystals (mean: 0.97 mm in length and 0.08 mm in width) than *Datangia* (mean: 0.64 mm in length and 0.06 mm in width) when comparing samples of similar shell size. *Latiproductus* has a similar microstructure to

Gigantoproductus sp. 1 and *Datangia* (i.e., short columnar and long columnar respectively) with smaller crystals and less crystal size variation (Fig. 6). *Gigantoproductus* sp. 1 and *Datangia* have thicker ventral valves with a higher amount of growth lines (~15–20) in comparison with *Latiproductus* (~5–8). Microstructural variations in crystal size between genera seem to be related to the variations of the ventral valve thickness, while the crystal shape seems to be genus-related.

Microstructures in gigantoproductid specimens illustrated in this study may be compared with those already reported in the literature, offering a novel taxonomic character for brachiopod systematics (Mii *et al.* 2001; Armendáriz *et al.* 2008; Angiolini

et al. 2012, 2019; Nolan 2017). However, big columnar crystals can be identified all *Gigantoproductus* specimens except in Armendáriz et al. (2008), which shows subhorizontal and short columnar crystals. Microstructure and shell thickness strongly suggest that taxa illustrated by Armendáriz et al. (2008) are *Globosoproductus* and *Latiproductus*.

Crystal size may be related to shell size differences because larger genera exhibit larger crystals, except for *Semiplanus*, which has longer crystals but with inclined orientations. The crystal size and orientation in each shell region may influence the external shape of the shell, although this relationship needs to be further investigated.

Brachiopod shells are assembled from numerous crystals of different sizes (length and width), probably related to the external shell morphology (i.e., spiral development), and clearly related to the different ontogenetic areas and hence to growth rates. Gigantoproductid microstructure shows that the largest crystals occur in thicker shell parts (e.g., Tk- and U-parts), and shorter crystals are situated in the thinnest and the innermost parts of the shell (T- and ITk-parts). Thick-shelled taxa (*Gigantoproductus* sp. 1 and *Datangia*) show more differences in crystal size between parts than thinner-shelled taxa (*Globosoproductus*, *Latiproductus* and *Semiplanus*), because the thickness variation across the shell is higher. *Gigantoproductus* sp. 2 valves exhibit intermediate crystal size variations between two groups.

Brachiopod shells have been classified in the literature in terms of the function of microstructure and geochemical differences between each valve (Pérez-Huerta & Reed 2018) or at intra-shell level; for instance the umbo is systematically enriched in magnesium (Buening & Carlson 1992). Differences in fibre sizes within the secondary shell layers of extant Terebratulida and Rhynchonellida, at different positions within the shell growth spiral, were reported by Ye et al. (2018). Larger fibres were systematically located towards the innermost part of the shell and this was interpreted by Ye et al. (2018) as an ontogenetic trend. Furthermore, crystal size differences have been reported in genera possessing shells of two- and three-layered construction, with the size of crystal fibres of the secondary layer being larger in genera with two-layered shells (Ye et al. 2018). In gigantoproductids, the tertiary layer represents almost the entire shell and influences the shell morphology (i.e., spiral development). The column elongation is sub-perpendicular to the shell surface, except in *Globosoproductus* (subhorizontal microstructure) and *Kansuella?* (crenulated), thus the crystal length of the tertiary layer is an optimal parameter to compare size trends among gigantoproductids. Crystal length (Fig. 7) ontogenetically varies, in a longitudinal growth trend, from one or two stages of short crystals at umbonal part, which rapidly increases its size towards the Tk-part and decreases towards commissure (T-part). In transverse growth crystal sizes decrease from the external and middle parts towards the internal parts (i.e., ITk- and IT-parts, respectively). These ontogenetic trends are different from those illustrated by Ye et al. (2018), which might be related to orientation differences in the elongation axis of columns, different regimes in shell secretion of the secondary and tertiary layer or lineage-specific differences (different brachiopod orders). The understanding of the shell morphology and thickness through the evolution of microstructural changes during the Viséan–Serpukhovian could be the key to understanding the environmental changes during the mid–Carboniferous.

5. Conclusions

- Taxonomic identifications of gigantoproductids from sections in southern Spain, southern France and central Morocco have been assessed in

Globosoproductus, *Kansuella?*, *Semiplanus*, *Latiproductus*, *Gigantoproductus* (G. sp. 1 and G. sp. 2) and *Datangia* using morphological criteria such as ribbing density, shell dimensions and shell morphology.

- Detailed microstructural characterisation of ventral valves shows that all valves consist of two preserved layers, laminar secondary and columnar tertiary, in which six different crystal morphologies in the tertiary layer are recognised: subhorizontal columnar morphology in *Globosoproductus*, imbricated columnar in *Semiplanus*, crenulated in *Kansuella?*, short columnar in *Latiproductus*, acicular columnar in *Gigantoproductus* sp. 2 and long columnar in *Gigantoproductus* sp. 1 and *Datangia*. These crystal morphologies in the tertiary layer are taxon-specific.
- Thicker-shelled genera (*Gigantoproductus* and *Datangia*) have higher variation in crystal size and higher crystal lengths than thinner-shelled genera (*Latiproductus*, *Globosoproductus* and *Semiplanus*), although shell spiral development is independent of shell thickness.
- During the Viséan–Serpukhovian interval gigantoproductid populations changed gradually from thinner-shelled with subhorizontal columnar morphology to a thicker-shelled genus with long columnar crystal morphology.
- Morphological comparison between shell characters plays an important role in brachiopod classification (Thomson 1927; Williams 1956). Some authors noted that juvenile brachiopod shells have few or even non-diagnostic characters of adult specimens; this fact stressed the need for ontogenetic information in taxonomic diagnoses and descriptions (Lee & Wilson 1979). The combination of tertiary layer microstructure, maximum shell thickness and the shell growth spiral seems to offer a robust taxonomic framework for gigantoproductid taxonomy, especially when key characters are obliterated by taphonomic processes (i.e., ribbing spacing and thickness, muscle scars, morphology of the cardinal process and median septum). These features are highly taxon-specific and may be measured in fragmented and complete samples, and are promising for application to the systematics of other brachiopod groups.

6. Acknowledgements

Financial support through the Spanish Ministerio de Economía y Competitividad (research projects CGL2012-30922BTE and CGL2016-78738-P) and the Complutense University Research Group (910231) is gratefully acknowledged. J.R.M.-C. acknowledges financial support through an FPI-MINECO grant. This article is a contribution to the Spanish Working Group IGCP 596 (UNESCO). We thank the anonymous reviewers and the editor for their corrections and suggestions, which improved an earlier version of this manuscript.

7. Competing interests

The author(s) declare none.

8. References

- Abramoff, M. D., Magalhães, P. J. & Ram, S. J. 2004. Image processing with ImageJ. *Biophotonics International* **11**, 36–42.
- Ackerly, S. C. 1992. Morphogenetic regulation in the shells of bivalves and brachiopods: evidence from the geometry of the spiral. *Lethaia* **25**, 249–56.
- Aldridge, A. E. 1999. Brachiopod outline and episodic growth. *Paleobiology* **25**, 471–82.
- Aldridge, A. E. & Gaspard, D. 2011. Brachiopod life histories from spiral deviations in shell shape and microstructural signature – preliminary report. *Memoirs of the Association of Australasian Palaeontologists* **41**, 257–68.
- Angiolini, L., Crippa, G., Azmy, K., Capitani, G., Confalonieri, G., Della Porta, G., Griesshaber, E., Harper, D. A. T., Leng, M. J., Nolan, L., Orlandi, M., Posenato, R., Schmahl, W. W., Banks, V. J. & Stephenson, M. H. 2019. The giants of the phylum Brachiopoda: a matter of diet? *Palaeontology* **62**, 889–917.
- Angiolini, L., Darbyshire, D. P. F., Stephenson, M. H., Leng, M. J., Brewer, T. S., Berra, F., Jadoul, F., Millward, D., Aldridge, A., Andrews, J., Chenery, S. & Williams, G. 2012. Heterogeneity, cyclicity and diagenesis in a Mississippian brachiopod shell of palaeo-equatorial Britain. *Terra Nova* **24**, 16–26.
- Aretz, M., Legrand-Blain, M., Vachard, D. & Izart, A. 2019. Gigantoproductid and allied productid brachiopods from the ‘Calcaires à Productus’ (late Viséan–Serpukhovian; Montagne Noire, southern France): taxonomy and palaeobiogeographical position in the Palaeotethys. *Geobios* **55**, 17–40.
- Armendáriz, M., Rosales, I. & Quesada, C. 2008. Oxygen isotope and Mg/Ca⁻¹ composition of Late Viséan (Mississippian) brachiopod shells from SW Iberia: palaeoclimatic and palaeogeographic implications in northern Gondwana. *Palaeogeography, Palaeoclimatology, Palaeoecology* **268**, 65–79.
- Balthasar, U., Jin, J., Hints, L. & Cusack, M. 2020. Brachiopod shell thickness links environment and evolution. *Palaeontology* **63**, 171–83.
- Baumgarten, S., Laudien, J., Jantzen, C., Häussermann, V. & Försterra, G. 2013. Population structure, growth and production of a recent brachiopod from the Chilean fjord region. *Marine Ecology* **35**, 401–13.
- Brunton, C. H. C. & Lazarev, S. S. 1997. Evolution and classification of the Productellidae (Productida), upper Paleozoic brachiopods. *Journal of Paleontology* **71**, 381–94.
- Brunton, C. H. C., Lazarev, S. S. & Grant, R. E. 1995. A review and new classification of the brachiopod order Productida. *Palaeontology* **38**, 915–36.
- Buening, N. & Carlson, S. J. 1992. Geochemical investigation of growth in selected extant articulate brachiopods. *Lethaia* **25**, 331–45.
- Cabanás, R. 1963. Contribución a los estudios del Carbonífero de los alrededores de Córdoba. *Breviora. Geológica Astúrica* **2**, 63–8.
- Chao, Y. T. 1928. Productidae of China, part II: Chonetinae, Productidae and Richthofeniinae. *Palaeontologica Sinica (Series B)* **5**, 1–103.
- Clark, J. V., Aldridge, A. E., Reolid, M., Endo, K. & Pérez-Huerta, A. 2015. Application of shell spiral deviation methodology to fossil brachiopods: implications for obtaining specimen ontogenetic age. *Palaeontologia Electronica* **18**, 1–39.
- Clark, J. V., Pérez-Huerta, A., Gillikin, D. P., Aldridge, A. E., Reolid, M. & Endo, K. 2016. Determination of paleoseasonality of fossil brachiopods using shell spiral deviations and chemical proxies. *Palaeoworld* **25**, 662–74.
- Conrad, J. & Legrand-Blain, M. 1971. *Titanaria africana* nov. sp., un nouveau Gigantoproductide du Namurien saharien. *Bulletin de la Société d'histoire naturelle de l'Afrique du Nord* **62**, 107–31.
- Cózar, P. 2004. Foraminiferal and algal evidence for the recognition of the Asbian/Brigantian boundary in the Guadiato area (Mississippian, southwestern Spain). *Revista Española de Micropaleontología* **36**, 367–88.
- Cózar, P., Rodríguez-Martínez, M., Falces, S., Mas, R. & Rodríguez, S. 2003. Stratigraphic setting in the development of microbial mud mounds of the lower Carboniferous of the Guadiato area (SW Spain). In Ahr, W. M., Harris, P. M., Morgan, W. A. & Somerville, I. D. (eds) *Permian Carboniferous carbonate platforms and reefs. Society of economic paleontologists and mineralogists*, 57–67. Tulsa: Special Publication 78, and American Association of Petroleum Geologists, Memoir 83.
- Cózar, P. & Rodríguez, S. 1999. Evolución sedimentaria del Carbonífero Inferior del Área del Guadiato (España). *Boletín Geológico y Minero* **110**, 663–80.
- Cózar, P. & Rodríguez, S. 2000. Caracterización estratigráfica y sedimentológica del Viséense superior de Sierra Boyera (área del Guadiato, SO de España). *Revista de la Sociedad Geológica de España* **13**, 91–104.
- Cózar, P. & Rodríguez, S. 2004. Pendleian (early Serpukhovian) marine carbonates from SW Spain: sedimentology, biostratigraphy and depositional model. *Geological Journal* **39**, 25–47.
- Cózar, P., Rodríguez, S., & Mas, R. (2004). Análisis sedimentológico y bioestratigráfico de afloramientos del Serpujoviense inferior (Mississippiense) en las proximidades de Adamuz (Córdoba, SO de España). *Coloquios de Paleontología*, **54**, 115–30
- Cózar, P., Said, I., Somerville, I. D., Vachard, D., Medina-Varea, P., Rodríguez, S. & Berkhli, M. 2011. Potential foraminiferal markers for the Viséan–Serpukhovian and Serpukhovian–Bashkirian boundaries – a case study from central Morocco. *Journal of Paleontology* **85**, 1105–27.
- Cózar, P., Somerville, I. D., Rodríguez, S., Mas, R. & Medina-Varea, P. 2006. Development of a late Viséan (Mississippian) mixed carbonate/siliciclastic platform in the Guadalquivir Valley (southwestern Spain). *Sedimentary Geology* **183**, 269–95.
- Cózar, P., Vachard, D., Izart, A., Said, I., Somerville, I., Rodríguez, S., Coronado, I., El Houicha, M. & Ouarhache, D. 2020. Lower-middle Viséan transgressive carbonates in Morocco: Palaeobiogeographic insights. *Journal of African Earth Sciences* **168**, 103850.
- Ferguson, J. 1978. Some aspects of the ecology and growth of the Carboniferous gigantoproductids. *Proceedings of the Yorkshire Geological Society* **42**, 41–54.
- Fielding, C. R., Frank, T. D., Birgenheier, L. P., Rygel, M. C., Jones, A. T. & Roberts, J. 2008. Stratigraphic imprint of the Late Palaeozoic Ice Age in eastern Australia: a record of alternating glacial and nonglacial climate regime. *Journal of the Geological Society* **165**, 129–40.
- Foster, M. W. 1974. Recent Antarctic and Subantarctic brachiopods. *Antarctic Research Series* **21**, 1–189.
- Garbelli, C. 2017. Shell microstructures in Upper Permian brachiopods: implication for fabric evolution and calcification. *Rivista Italiana di Paleontologia e Stratigrafia* **123**, 541–60.
- Gaspard, D., Aldridge, A. E., Boudouma, O., Fialin, M., Rividi, N. & Lécuyer, C. 2018. Analysis of growth and form in *Aerothyris kerguelenensis* (rhynchonelliform brachiopod) – shell spiral deviations, microstructure, trace element contents and stable isotope ratios. *Chemical Geology* **483**, 474–90.
- González, F., Rodríguez-Castro I. & Rodríguez, S. 2018. Palinomorfos Misisípicos del Área del Guadiato. Datos preliminares. Conference paper at XXXIV Jornadas de la Sociedad Española de Paleontología. In Vaz, N. & Sá, A.A. (eds) *Yacimientos paleontológicos excepcionales en la península Ibérica. Cuadernos del Museo Geominero (27)*, 449–54. Madrid: Instituto Geológico y Minero de España.
- Griesshaber, E., Schmahl, W. W., Neuser, R., Pettke, T., Blum, M., Mutterlose, J. & Brand, U. 2007. Crystallographic texture and microstructure of terebratulide brachiopod shell calcite: an optimized materials design with hierarchical architecture. *American Mineralogist* **92**, 722–34.
- Hiller, N. 1988. The development of growth lines on articulate brachiopods. *Lethaia* **21**, 177–88.
- Ibaraki, Y., Tazawa, J., Sato, K. & Nakamura, Y. 2008. *Gigantoproductus* (Carboniferous Brachiopoda) from Kotaki, Itoigawa City, Niigata Prefecture, central Japan. *Science Reports, Niigata University (Geology)* **23**, 55–64.
- Kowalewski, M., Dyreson, E., Marcot, J. D., Vargas, J. A., Flessa, K. W. & Hallman, D. P. 1997. Phenetic discrimination of biometric complexes: paleobiological implications of morphospecies in the lingulide brachiopod *Glottidia*. *Paleobiology* **23**, 444–69.
- Lazarev, S. S. 1990. Evolution and systematics of the productids. *Trudy Paleontologicheskii Institut* **242**, 1–174 (in Russian).
- Lee, D. E. & Wilson, J. B. 1979. Cenozoic and extant rhynchonellide brachiopods of New Zealand: systematics and variation in the genus *Notosaria*. *Journal of the Royal Society of New Zealand* **9**, 437–63.
- Legrand-Blain, M. 1973. Les Gigantoproductides (brachiopodes) du Sahara algérien I. – Gigantoproductides Viséens. *Bulletin de la Société d'histoire naturelle de l'Afrique du Nord, Alger* **64**, 79–158.
- Legrand-Blain, M. 1980. Les Gigantoproductides (brachiopodes) du Sahara Algérien. III – Semiplanidae viséens et namuriens. *Bulletin de la Société d'histoire naturelle de l'Afrique du Nord* **69**, 1–2.
- Legrand-Blain, M. 1985. Brachiopods. In Wagner, R. H., Winkler Prins, C. F. & Granados, L. F. (eds), *Carboniferous of the world. 2. Australia, Indian subcontinent, South Africa, South America and North Africa*, 372–4. Madrid: IGME.
- Legrand-Blain, M. 1987. Les Gigantoproductidae (brachiopodes) namuriens du Sahara algérien. *Bulletin de la Société belge de Géologie* **96**, 159–94.

- Legrand-Blain, M., Devolvé, J. & Perret, M. 1983. Les brachiopodes carbonifères des Pyrénées centrales françaises. I: Cadre stratigraphique et sédimentaire ; étude des Strophomenida. *Geobios* **16**, 285–327.
- Litvinovich, N. V. & Vorontsova, T. N. 1983. The question of the revision of *Gigantoproductus* Prentice. *Bulleten Moskovskogo Obshchestva Ispytatelei Prirody (MOIP), Otdelenie Geologicheskii* **58**, 81–94 (in Russian).
- Manceñido, M. O. & Motchurova-Dekova, N. 2010. A review of the crural types, their relationships to shell microstructure, and significance among post-Palaeozoic Rhynchonellida. *Special Papers in Palaeontology* **84**, 203–24.
- Martínez-Chacón, M. L. & Legrand-Blain, M. 1992. Braquiópodos. *Coloquios de Paleontología* **44**, 91–144.
- McGhee, Jr., G. R. 2001. The ‘multiple impacts hypothesis’ for mass extinction: a comparison of the Late Devonian and the late Eocene. *Palaeogeography, Palaeoclimatology, Palaeoecology* **176**, 47–58.
- Mii, H. S., Grossman, E. L., Yancey, T. E., Chuvashov, B. & Egorov, A. 2001. Isotopic records of brachiopod shells from the Russian Platform – evidence for the onset of mid-carboniferous glaciation. *Chemical Geology* **175**, 133–47.
- Moreno-Eiris, E., Perejón, A., Rodríguez, S. & Falces, S. 1995. Field Trip D. Palaeozoic Cnidaria and Porifera from Sierra Morena. In Perejón, A. (ed.) *VII International symposium on fossil cnidaria and Porifera*, 1–68. Madrid: Universidad Complutense.
- Motchurova-Dekova, N. 2001. Taxonomic and phylogenetic aspects of the shell ultrastructure of nine Cretaceous rhynchonellid brachiopod genera. *Paleontological Research* **5**, 319–30.
- Motchurova-Dekova, N., Saito, M. & Endo, K. 2002. The recent Rhynchonellid brachiopod *Parasphenaria cavernicola* gen. et sp. nov. from the submarine caves of Okinawa, Japan. *Paleontological Research* **6**, 299–319.
- Mottin, T., Iannuzzi, R., Vesely, F., Montañez, I., Griffis, N., Canata, R., Mairink Barão, L., Silveira, D. & Garcia, A. 2022. A glimpse of a Gondwanan postglacial fossil forest. *Palaeogeography, Palaeoclimatology, Palaeoecology* **588**, 110814.
- Muir-Wood, H. M. & Cooper, G. A. 1960. Morphology, classification and life habits of the Productoidea (Brachiopoda). *Geological Society of America Memoir* **81**, 447 pp.
- Nolan, L. S. P. 2017. *Equatorial sea surface temperature seasonality in the Mississippian (Carboniferous) derived from brachiopod shell calcite*. PhD thesis, University of Leicester, UK. 208 pp.
- Nolan, L. S. P., Angiolini, L., Jadoul, F., Della Porta, G., Davies, S. J., Banks, V. J., Stephenson, M. H. & Leng, M. J. 2017. Sedimentary context and palaeoecology of *Gigantoproductus* shell beds in the Mississippian Eyam Limestone Formation, Derbyshire carbonate platform, central England. *Proceedings of the Yorkshire Geological Society* **61**, 239–57.
- Paine, R. T. 1969. Growth and size distribution of the brachiopod *Terebratalia transversa* Sowerby. *Pacific Science* **23**, 337–43.
- Pakhnevich, A. V. 2019. Shell Interior of *Semiplanella carinthica* Sarycheva et Legrand-Blain (Brachiopoda, Productida). *Paleontological Journal* **53**, 132–9.
- Pattison, J. 1981. *The stratigraphical distribution of gigantoproductoid brachiopods in the Viséan and Namurian rocks of some areas in northern England* **81**, 1–30. London: Institute of Geological Sciences.
- Pérez-Huerta, A., Aldridge, A. E., Endo, K. & Jeffries, T. E. 2014. Brachiopod shell spiral deviations (SSD): implications for trace element proxies. *Chemical Geology* **374**, 13–24.
- Pérez-Huerta, A., Coronado, I., & Hegna, T. A. (2018). Understanding biomineralization in the fossil record. *Earth-Science Reviews*, **179**, 95–122.
- Pérez-Huerta, A. & Reed, H. 2018. Preliminary assessment of coupling the analysis of shell microstructures and microtextures as palaeoecological indicator in fossil brachiopods. *Spanish Journal of Palaeontology* **33**, 129–38.
- Prentice, J. E. 1950. The genus *Gigantella* Sarycheva. *Geological Magazine* **87**, 436–8.
- Prentice, J. E. 1956. *Gigantoproductus edelburgensis* (Phillips) and related species. *Proceedings of the Yorkshire Geological Society* **30**, 229–58.
- Qiao, L. & Shen, S. Z. 2012. Late Mississippian (Early Carboniferous) brachiopods from the western Daba Mountains, central China. *Alcheringa* **36**, 287–307.
- Qiao, L. & Shen, S. Z. 2015. A global review of the Late Mississippian (Carboniferous) *Gigantoproductus* (Brachiopoda) faunas and their paleogeographical, paleoecological, and paleoclimatic implications. *Palaeogeography, Palaeoclimatology, Palaeoecology* **420**, 128–37.
- Radulović, B., Motchurova-Dekova, N. & Radulović, V. 2007. New Barremian rhynchonellid brachiopod from Serbia and the shell microstructure of Tetrarhynchiidae. *Acta Palaeontologica Polonica* **52**, 761–82.
- Rodríguez, S., Arribas, M. E., Comas-Rengifo, M. J., de la Peña, J. A., Falces, S., Gegúndez, P., Kullman, J., Legrand-Blain, M., Martínez-Chacón, M. L., Moreno-Eiris, E., Perejón, A., Sánchez, J. L., Sánchez-Chico, F. & Sarmiento, G. 1992. Análisis paleontológico y sedimentológico de la cuenca carbonífera de Los Santos de Maimona (Badajoz). *Coloquios de Paleontología* **44**, 12–32.
- Rodríguez, S. & Comas-Rengifo, M. J. (1989). Los Heterocorales del carbonífero de los Santos de Maimona (Badajoz, SW de España). *Coloquios de Paleontología*, 61–82.
- Rudwick, M. J. 1959. The growth and form of brachiopod shells. *Geological Magazine* **96**, 1–24.
- Rush, P. F. & Chafetz, H. S. 1990. Fabric-retentive, non-luminescent brachiopods as indicators of original $\delta^{13}\text{C}$ and $\delta^{18}\text{O}$ composition; a test. *Journal of Sedimentary Research* **60**, 968–81.
- Sarycheva, T. G. 1928. Podmoskovnye produktivny gruppy *Productus giganteus* Mart. (*Gigantella* gen. nov.). *Trudy Geologii Nauchno-Issledovatel'skii Institut, Geologii i Mineralnogo syrya (Saigims), Izdatel'stvo 'Fan' Uzbekskoi SSR, Tashkent* **1**, 1–71 (in Russian).
- Sarycheva, T. G. & Legrand-Blain, M. 1977. Generic composition and evolution of the family Semiplanidae (Brachiopoda). *Paleontologicheskii Zhurnal* **1977**, 70–82 (in Russian; English translation in *Paleontological Journal* 1977, 200–12).
- Sarycheva, T. G. & Sokolskaya, A. N. 1952. Description of Palaeozoic Brachiopoda of the Moscow Basin. *Akademiya Nauk SSSR, Paleontologicheskii Institut, Trudy* **38**, 1–307 (in Russian).
- Simonet-Roda, M., Griesshaber, E., Angiolini, L., Harper, D. A. T., Jansen, U., Bitner, M. A., Henkel, D., Manzanero, E., Muller, T., Tomašových, A., Eisenhauer, A., Ziegler, A. & Schmahl, W. W. 2021. The evolution of the tectonide microstructures and textures: traced from Triassic to Holocene. *Lethaia* **54**, 558–77.
- Simonet-Roda, M., Ziegler, A., Griesshaber, E., Yin, X., Rupp, U., Greiner, M., Henkel, D., Häussermann, V., Eisenhauer, A., Laudien, J. & Schmahl, W. W. 2019. Terebratulid brachiopod shell biomineralisation by mantle epithelial cells. *Journal of Structural Biology* **207**, 136–57.
- Smirnova, T. N. & Zhegallo, E. A. 2022. The acretroid type of shell microstructure in the genus *Kasagittella* (Order Lingulida) from the Upper Devonian of the Volga-Urals Region. *Paleontological Journal* **56**, 47–51.
- Tazawa, J. & Miyake, Y. 2002. *Gigantoproductus* (Brachiopoda) from the Lower Carboniferous (Upper Viséan) Onimaru Formation of the southern Kitakami Mountains, NE Japan. *Science Report, Niigata University, Serie E (Geology)* **17**, 1–6.
- Thomson, J. A. 1927. Brachiopod morphology and genera (recent and tertiary). *New Zealand Board of Science and Art Manual* **7**, 1–338.
- Vachard, D., Cózar, P., Aretz, M. & Izart, A. 2016. Late Viséan–Serpukhovian foraminifers in the Montagne Noire (France): biostratigraphic revision and correlation with the Russian substages. *Geobios* **49**, 469–98.
- Vachard, D., Izart, A. & Cózar, P. 2017. Mississippian (middle Tournaisian–late Serpukhovian) lithostratigraphic and tectonosedimentary units of the southeastern Montagne Noire (Hérault, France). *Géologie de la France* **1**, 47–88.
- Vermeij, G. J. 2016. Gigantism and its implications for the history of life. *PLoS ONE* **11**, e0146092.
- Vischer, N., Huls, P. & Woldringh, C. 1994. Object-Image: an interactive image analysis program using structured point collection. *Binary* **6**, 160–6.
- Watson, S. A., Peck, L. S., Tyler, P. A., Southgate, P. C., Tan, K. S., Day, R. W. & Morley, S. A. 2012. Marine invertebrate skeleton size varies with latitude, temperature and carbonate saturation: implications for global change and ocean acidification. *Global Change Biology* **18**, 3026–38.
- Williams, A. 1956. The calcareous shell of the Brachiopoda and its importance to their classification. *Cambridge Philosophical Society, Biological Reviews* **31**, 243–87.
- Williams, A. 1968. Evolution of the shell structure of articulate brachiopods. *Palaeontological Association Special Paper* **2**, 1–55.
- Williams, A., Brunton, C. H. C., Carlson, S. J., Alvarez, F., Ansell, A. D., Baker, P. G., Bassett, M. G., Blodgett, R. B., Boucot, A. J., Carter, J. L., Cocks, L. R. M., Cohen, B. L., Copper, P., Curry, G. B., Cusack, M., Dags, A. S., Emig, C. C., Gawthrop, A. B., Gourvennec, R., Grant, R. E., Harper, D. A. T., Holmer, L. E., Hou, H.-F., James, M. A., Jin, Y.-G., Johnson, J. G., Laurie, J. R., Lazarev, S., Lee, D. E., Lüter, C., Mackay, S., MacKinnon, D. I., Manceñido, M. O., Mergl, M., Owen, E. F., Peck, L. S., Popov, L. E., Racheboeuf, P. R., Rhodes, M. C., Richardson, J. R., Rong, J.-Y., Rubel, M., Savage, N. M., Smirnova, T. N., Sun D.-L., Walton, D., Wardlaw, B. & Wright, A. D. 2007. Treatise on Invertebrate Palaeontology (Part H, Brachiopoda revised). Vol. 3: *Linguliformea, Cratiformea, and Rhynchonelliformea*. Geological Society of America, Boulder, and University of Kansas Press, Lawrence.

- Williams, A., Carlson, S. J., Brunton, C. H. C., Holmer, L. E. & Popov, L. E. 1996. A supra-ordinal classification of the Brachiopoda. *Philosophical Transactions of the Royal Society of London (series B)* **351**, 1171–93.
- Yang, D., Ni, S., Chang, M. & Zhao, R. 1977. Brachiopoda. *Paleontological atlas of south central China, Late Paleozoic part 2*. Peking: Geological Publishing House.
- Ye, F., Crippa, G., Angiolini, L., Brand, U., Capitani, G., Cusack, M., Garbelli, C., Grieshaber, E., Harper, E. & Schmahl, W. 2018. Mapping of extant brachiopod microstructure: a tool for environmental studies. *Journal of Structural Biology* **201**, 221–36.
- Zakowa, H. 1985. Upper Viséan gigantoproductoid brachiopods from the Gory Swietokrzyskie, Poland. *Annales Societatis Geologorum Poloniae* **55**, 105–26.
- Zhang, Z., Augustin, M. & Payne, J. L. 2015. Phanerozoic trends in brachiopod body size from synoptic data. *Paleobiology* **41**, 491–501.

MS received 30 April 2022. Accepted for publication 21 September 2022. First published online 21 October 2022